Table 1. Tumor initiation capability of $CD271^+$ cells vs, $CD271^-$ cells.

	Population	Number of cells injected	Weeks				
			2	4	6	8	10
HPCM1	$CD271^+$	30	0/6	**1/6**	**2/6**	**4/6**	**4/6**
	$CD271^-$	30	0/6	0/6	0/6	0/6	**1/6**
	$CD271^+$	100	0/4	**1/4**	**3/4**	**3/4**	**3/4**
	$CD271^-$	100	0/4	0/4	0/4	0/4	0/4
	$CD271^+$	300	0/4	**1/4**	**4/4**	**4/4**	**4/4**
	$CD271^-$	300	0/4	0/4	0/4	0/4	0/4
	$CD271^+$	1,000	0/2	**1/2**	**2/2**	**2/2**	**2/2**
	$CD271^-$	1,000	0/2	0/2	**2/2**	**2/2**	**2/2**
HPCM2	$CD271^+$	100	0/4	0/4	0/4	0/4	0/4
	$CD271^-$	100	0/4	0/4	0/4	0/4	0/4
	$CD271^+$	300	0/6	0/6	0/6	**1/6**	**1/6**
	$CD271^-$	300	0/6	0/6	0/6	0/6	0/6
	$CD271^+$	1,000	0/8	**1/8**	**2/8**	**4/8**	**4/8**
	$CD271^-$	1,000	0/8	0/8	**1/8**	**1/8**	**1/8**
	$CD271^+$	10,000	0/2	**1/2**	**1/2**	**1/2**	**1/2**
	$CD271^-$	10,000	0/2	0/2	0/2	0/2	0/2
HPCM3	$CD271^+$	300	0/4	0/4	**1/4**	**2/4**	**3/4**
	$CD271^-$	300	0/4	0/4	**1/4**	**1/4**	**1/4**
	$CD271^+$	1,000	0/4	0/4	**3/4**	**4/4**	**4/4**
	$CD271^-$	1,000	0/4	0/4	0/4	**2/4**	**2/4**
	$CD271^+$	10,000	0/4	0/4	**4/4**	**4/4**	**4/4**
	$CD271^-$	10,000	0/4	0/4	0/4	**3/4**	**4/4**
	$CD271^+$	100,000	0/2	**2/2**	**2/2**	**2/2**	**2/2**
	$CD271^-$	100,000	0/2	0/2	**2/2**	**2/2**	**2/2**

doi:10.1371/journal.pone.0062002.t001

suggested that the $CD271^+$ cells are armed with MMPs that enable tissue invasion by breaking down the extracellular matrix.

$CD271^+$ Cells are Chemoresistant *in vivo*

To determine whether the $CD271^+$ population is chemoresistant, the effect of CDDP on the cells was analyzed. Our initial *in vitro* analysis failed, due to difficulty in tissue culture maintenance, either under regular tissue culture conditions with serum or under serum-free sphere culture conditions (data not shown). Therefore, we used an *in vivo* evaluation model. Mice bearing HPCM1-derived tumors were treated with CDDP, and on day 7, the tumors were resected, sectioned, and examined by IHC for CD271 (**Figure 4A**). The flattened and keratinized $CD271^-$ cells in the central zone of the tumor were in the process of dying, suggesting that chemotherapy had caused massive necrosis in these cells (**Figure 4A**). In contrast, as was most apparent in the basal layer, $CD271^+$ cells survived and were surrounded by stroma. To verify that the $CD271^+$ cells were refractory to CDDP, a single-cell suspension prepared from a CDDP-treated tumor was analyzed by FACS (**Figure 4B**). After CDDP administration, the $CD271^+$ population increased from 16.3% to 35.2%, suggesting that the $CD271^+$ cells were resistant to CDDP. The multi-drug resistance of CSCs is attributed to an elevated expression of ATP-binding transporters [19], for example, ABCC2 contributes to the efflux of CDDP and docetaxel, and ABCB5 and ABCG2 contribute to the efflux of 5-FU. We therefore compared the expression of these three ATP-binding transporters in the $CD271^+$ and $CD271^-$ cells of HPCM1 (**Figure 4C**). The expression of *ABCC2*, *ABCB5*, and *ABCG2* in the $CD271^+$ cells was about 2.5-fold, 4.8-fold, and 2.4-fold higher than that in the $CD271^-$ cells, respectively. Together, these results indicated that the $CD271^+$ cells are chemoresistant.

CD271 Expression in HPC Clinical Specimens is Correlated with a Poor Prognosis

To investigate whether CD271 expression was associated with any prognostic factors for primary HPC patients, 83 clinical specimens obtained from surgery or biopsy were examined for CD271. For this evaluation, because the $CD271^+$ cells were heterogeneously located within each tumor, we used a grading system that classified each case as either "strong," if it had more than 50% $CD271^+$ cells in the entire tumor, or "moderate-to-weak," if it had less than 50%. All the slides were evaluated independently by two investigators (I. S. and K. M.) without any prior knowledge of each patient's clinical information. By IHC staining of the HPC tissue specimens with an anti-CD271 antibody, 36 of the 83 cases were classified as strong, and 47 were moderate-to-weak (**Figure 5A**). The clinical and pathological characteristics of the 83 patients are summarized in **Table S3**. The CD271 grade was analyzed statistically with respect to the clinical T-stage, N-stage, and the stage of disease. The percentages of cancers at the advanced T stage (T3 or more) and advanced N stage (N2 or more) were significantly higher in the CD271 strong group than in the moderate-to-weak group (47.2% vs 23.4%: $p = 0.023$, and 69.4% vs 40.4%: $p = 0.009$, respectively). Similarly, cases of advanced disease (stage III and IV) were more frequent in the CD271 strong group than in the moderate-to-weak group (80.6% vs 55.3%: $p = 0.016$). Next, the disease-specific survival rate was compared using Kaplan-Meier methods. The three-year survival rate was significantly lower in the CD271 strong group compared to the CD271 moderate-to-weak group (54.3% vs 83.2%: $p = 0.043$) (**Figure 5B**). These data indicate that the histological expression of CD271 is associated with poor clinical outcomes.

We further examined whether the *CD271* gene expression in clinical specimens was associated with patients' prognosis. For this analysis, 28 cases of HPC that were completely resected, as assessed both surgically and histologically, were examined for *CD271* expression. Immediately after resection, each specimen was separated into tumor and normal hypopharyngeal mucosa. The total RNAs purified from these respective tissues, were subjected to *CD271* mRNA quantification. Because normal mucosa also expresses CD271 (**Figure 1C**), we used a "CD271-expression index," the value of *CD271* in tumor versus that in normal mucosa, as the CD271 level. During the average 20-month follow-up period, 11 of the 28 cases relapsed. All of the relapses occurred within 18 months, and the relapse-free survival for 18 months was analyzed using Kaplan-Meier methods (**Figure 6A**). Using a cut-off value for the CD271-expression index of 1.5, the *CD271*-high expressers relapsed significantly more frequently than the *CD271*-low cases (41.1% vs 80.0% relapse-free survival, respectively: $p = 0.035$). The demographic and clinical characteristics of these patients are shown in **Table S4**. For the clinical disease classification, pT3 or more was significantly more frequent in the CD271-high cases (CD271-high 15/17, CD271-low 5/11; $p = 0.022$). Taken together, these results indicated that CD271 expression is associated with poor clinical outcomes in terms of prognosis and relapse.

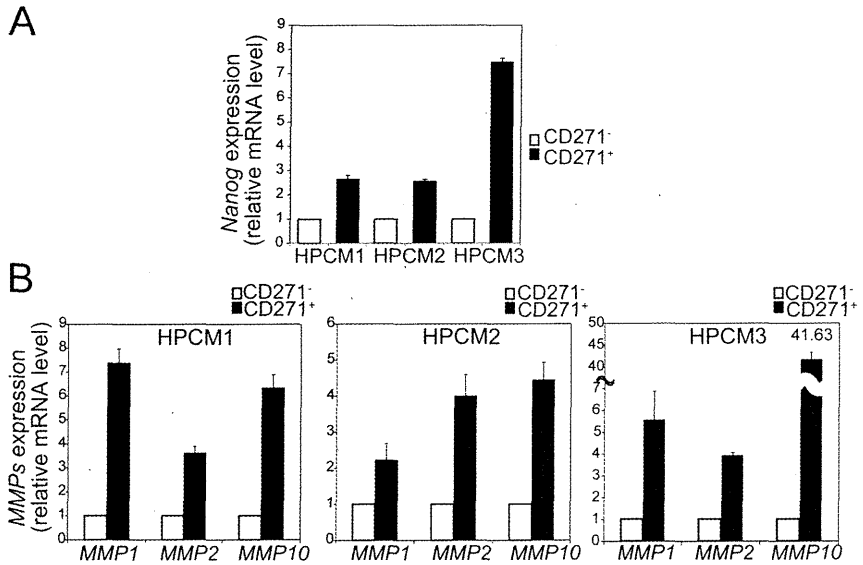

Figure 3. Expression profile of Nanog and MMPs in CD271$^+$ and CD271$^-$ cells. *Nanog* expression (A) and *MMP1, MMP2,* and *MMP10* expression (B) in CD271$^+$ and CD271$^-$ cells derived from the three HPC lines were analyzed by real-time RT-PCR. The transcript levels were normalized to those for *GAPDH,* and the fold change in the MMP expression level in CD271$^+$ cells versus CD271$^-$ cells was calculated for each sample. Values are the mean±SD of triplicate experiments.
doi:10.1371/journal.pone.0062002.g003

Nanog Expression is Associated with CD271 High Tumors

Next, because the *CD271* expression in HPC tumors had a positive relationship with that of *Nanog,* the *Nanog* expression in the same set of 28 clinical samples was quantified and analyzed. There was a significant association between the *CD271*-expression index and the *Nanog* index, which was the level of *Nanog* mRNA in the tumor versus that in normal mucosa (**Figure 6B**). Using a cut-off score 1.5 for the *Nanog* index, all the *Nanog*-high expressers (8 cases) were categorized into the *CD271*-high group. Taken together, these results suggest that both CD271 and *Nanog* are strong prognostic factors for HPC.

Discussion

The identification of cell-surface markers to define CSCs/CICs is important for the possible establishment of target-specific therapies using small molecule inhibitors and/or humanized antibodies. In this report, we show that the CD271$^+$ cells in HPC possess tumor-initiating capability *in vivo.* The CD271$^+$ cells are endowed with several CSC-like characteristics, including 1) tumor initiation, 2) high expression of the CSC-related gene *Nanog,* 3) self-renewal and the capacity to generate hierarchical populations, 4) chemoresistance, and 5) invasion capacity. Furthermore, we demonstrated that the expression of CD271 in HPC tumors is associated with a poor prognosis for HPC patients.

CSCs were first identified in acute myeloid leukemia (AML). A small subpopulation of AML cells with the CD34$^+$CD38$^-$ phenotype was observed to initiate tumors in immunodeficient mice [20]. Since then, xenograft models using highly immunodeficient mice have become widely used to evaluate the cancer stem cells within clinical cancer specimens, and xenotransplantation is currently regarded as the "gold standard" in this field [21]. Using this assay system, a number of solid tumors have been analyzed. Breast cancer cells with CD44$^+$CD24$^-$ were identified as CSCs, which form heterogeneous tumors with CD44$^{+/-}$ and CD24$^{+/-}$ phylogeny [22]. For HNSCC, only two reports have analyzed clinical specimen-based CSCs using xenotransplantation. Prince et al demonstrated that 5,000 CD44$^+$ cells could initiate a tumor [7], whereas Clay et al. demonstrated that 500 ALDH$^+$ cells formed a tumor [23]. Because positivity for ALDH is based on its enzyme activity, CD44 has been the cell-surface CSC marker studied in most detail. The same xenotransplantation methodology led to the characterization of CD133 as a laryngeal cancer stem cell marker using Hep-2 cells [24]. However, the CD133$^+$ cells from clinical HNSCC specimens have not been analyzed by xenotransplantation.

In our three primary HPC cases, CD133 expression was negative, as judged by FACS analyses and IHC (data not shown). Instead, we compared two independent subpopulations, CD44$^+$ and CD44$^-$. However, no significant difference was observed in the tumor-initiating capability of these populations *in vivo*; a minimum of 100 cells from either population initiated tumors (**Table S5**). Furthermore, a recent report showed that both the CD44$^-$ and CD44$^+$ cells of clinical HNSCC specimens possess similar sphere-forming and tumor-initiating capabilities, as well as chemoresistance [8]. Our results are consistent with this notion, with regard to the tumor-initiating capability.

Although categorized as HNSCC, HPC may have independent characteristics from other HNSCCs, especially with regard to the CSCs. Indeed, CSC markers are divergent, depending on the type of cancer. For example, CD44$^+$CD24$^-$ indicates breast cancer stem cells [22], whereas a pancreatic cancer stem cell phenotype is CD44$^+$CD24$^+$ [25], and CD44$^+$CD117$^+$ is an ovarian cancer stem cell phenotype [26]. Breast cancers, for instance, are classified into several subtypes, such as luminal, basal, and HER2$^+$, but the well-known CD44$^+$CD24$^-$ phenotype is closely associated with the basal type, and the HER2$^+$-type CSCs show an ALDH$^+$ phenotype [27]. Thus, since each cancer expresses a unique pattern of CSC markers, the CSC markers may also differ among types of HNSCCs.

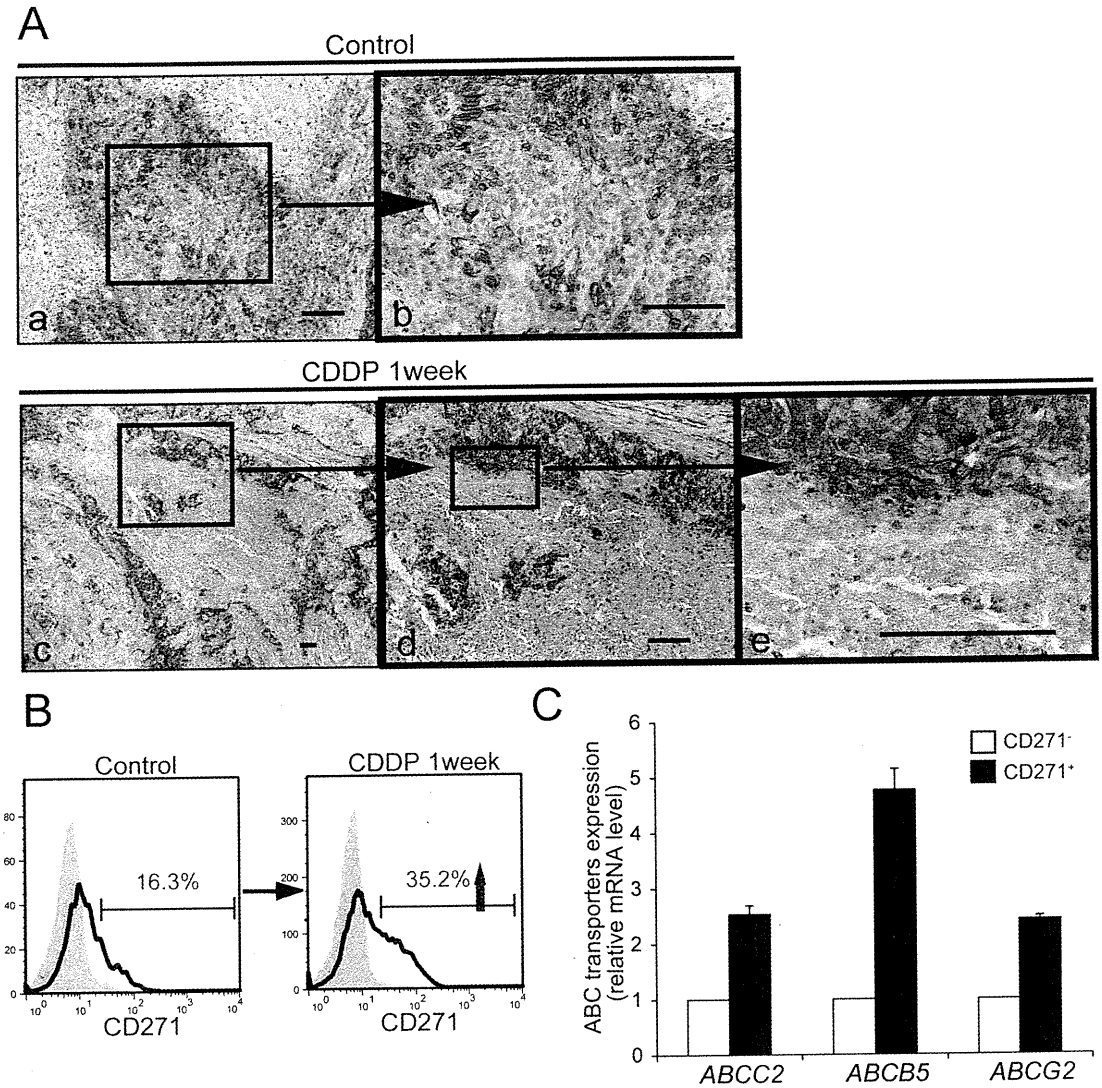

Figure 4. In vivo Chemoresistance of CD271$^+$ cells. (A) HPCM1- transplanted mice were treated with 7.5 mg/kg of CDDP for a week, then the generated tumors were analyzed by IHC for CD271. Boxed areas are linked to their respective high-magnification images by horizontal arrows. Scale bar: 100 μm. (B) FACS analyses for CD271 in HPCM1 cells derived from mice with or without CDDP treatment. (C) Expression of *ABCC2*, *ABCB5*, and *ABCG2* in CD271$^+$ and CD271$^-$ cells analyzed by real-time RT-PCR. Transcript levels were normalized to those of *GAPDH*, and the fold increase of each gene expression levels in CD271$^+$ cells versus CD271$^-$ cells are shown. Values are the mean±SD of triplicate experiments.
doi:10.1371/journal.pone.0062002.g004

In a variety of cancers, the CSCs are considered to be derived from the stem cells of normal tissues or from cancer cells acquiring stem cell pluripotency by accumulating genetic mutations [6]. Previous studies indicated that CD271 is expressed in tissue stem cells. In normal oral [11], laryngeal [12], and esophageal mucosa [13], CD271$^+$ cells are distributed in the basal layer. These observations are consistent with our present finding that CD271$^+$ cells were distributed in the basal layer of normal hypopharyngeal mucosa. Based on the hypothesis that CD271 is a tissue stem cell marker of the head and neck region, it is tempting to speculate that HPC CSCs are derived from the stem cells of normal mucosa.

In the present study, we observed that the CD271$^+$ cells of HPC possessed several characteristics of CSCs. First, the CD271$^+$ expression ranged from 2 to 20% of the tumor cells. Second, CD271$^+$ cells were more tumorigenic than CD271$^-$ cells. Third, the CD271$^+$ cells generated tumors that showed a striking similarity to the original ones *in vivo*, in which a heterogeneous population of CD271$^+$ and CD271$^-$ cells was present. These results indicated that the CD271$^+$ CSCs of HPC might originate from normal stem cells of the hypopharyngeal mucosa. Accordingly, recent reports propose that CD271 is a CSC marker of squamous cell carcinomas of esophageal origin [16] as well as malignant melanoma [14,15].

Accumulating evidence suggests that some CSCs reside close to blood vessels, in the perivascular niche [28,29]. In this regard, Krishnamurthy et al. demonstrated that the ALDH$^+$ cells of

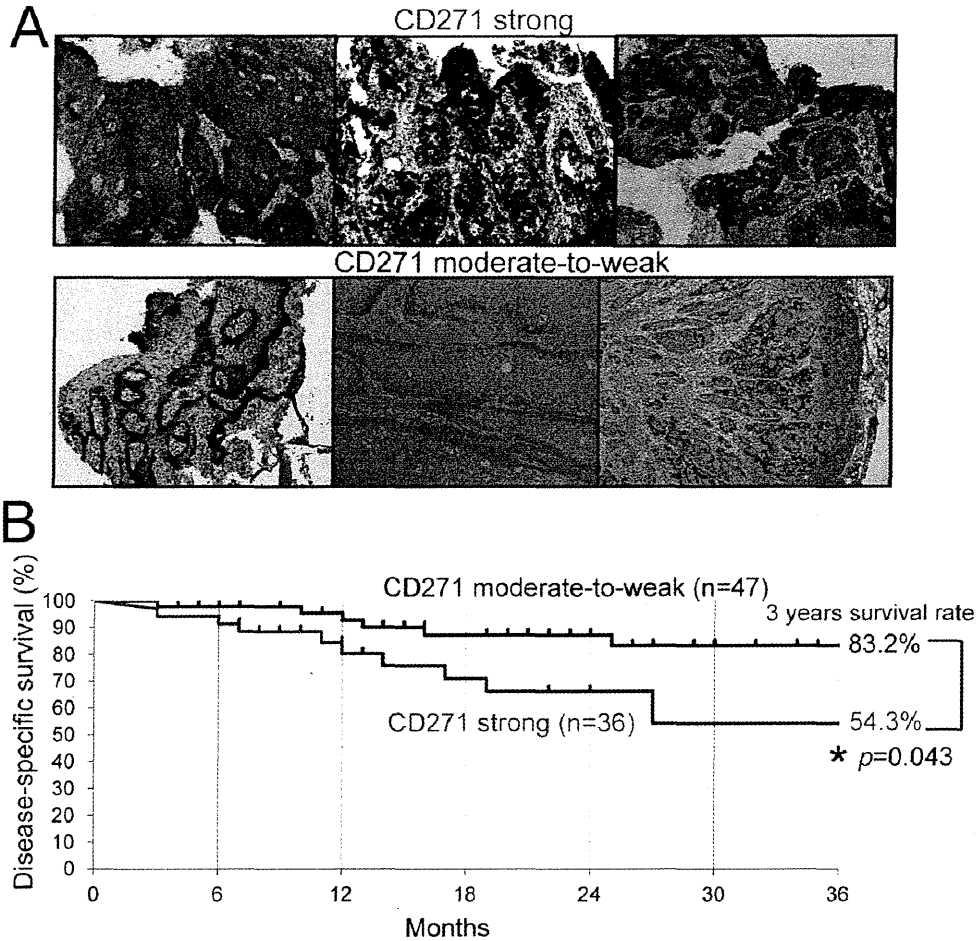

Figure 5. CD271 expression in HPC clinical specimens and progression of HPC patients. (A) Representative results of IHC analyses for CD271 in clinical specimens obtained from 83 HPC patients by surgery or biopsy. Immunopositivity appears brown. Specimens with more than 50% positive cells in the entire tumor were classified as "strong" (top), and less than 50%, as "moderate-to-weak" (bottom). (B) Kaplan-Meier analysis for the disease-specific survival rate (3 years) of the "strong" and "moderate-to-weak" groups. *Statistically significant.
doi:10.1371/journal.pone.0062002.g005

HNSCC are located within a 100-μm radius of blood vessels. The selective ablation of endothelial cells reduced the fraction of $CD44^+ALDH^+$ cells, suggesting that endothelial cells may form a microenvironment, or niche, that allows CSC survival and self-renewal [30]. In our analyses, the localization of $CD271^+$ HPC cells indicated that they might have been in direct contact with blood vessels, suggesting that either direct cell-to-cell interaction or some paracrine factor may promote the survival of CSCs. One interesting possibility is neurotrophins such as NGF support $CD271^+$ cells. The perivascular niche hypothesis needs to be further investigated by examining the $CD271^+$ cells' fate in HPC.

We also observed in the current study that $CD271^+$ cells were clustered within the invasive front area. The invasive front is the part of a growing tumor that extends most deeply into the adjacent non-cancerous tissue, and it is the location of the tumor-host communication interface [31–33]. Histopathological grading analyses revealed that the invasive front reflects the biological aggressiveness of a carcinoma [33]. In some of our specimens, $CD271^+$ cells formed small foci, which might be potential points of invasion initiation (**Figure 1C–c,d**). In accordance with this finding, the expressions of *MMP1*, *MMP2*, and *MMP10* were elevated in the $CD271^+$ cells. Because these secreted *MMPs* cleave the extracellular matrix, they are essential factors for invasion [31,34]. MMPs have been shown to contribute to tumorigenicity; the over-expression of *MMP1* enhances tumorigenicity, while its knockdown reduces tumor formation in a glioblastoma cell line [35]. In non-small cell lung cancers, MMP10 plays a pertinent role in tumor initiation, and it maintains the characteristics of CSCs [36]. Considering these reports, it is reasonable that MMP-positive $CD271^+$ cells show strong invasion capability as well as the potential to initiate tumors.

Nanog is one of the homeobox transcription factors expressed in pluripotent embryonic stem cells [37,38], and accumulating evidence suggests it has a role in inducing the pluripotency of various types of cancer. The over-expression of *Nanog* leads to elevated tumorigenicity [39,40], while its inhibition reduces tumorigenicity in prostate, breast, and colorectal cancers [39,41]. In HNSCC, sphere culture enhances the expression of *Nanog*, and in clinically dissected samples, high *Nanog* expression is closely associated with a poor prognosis for the patient [42]. In our

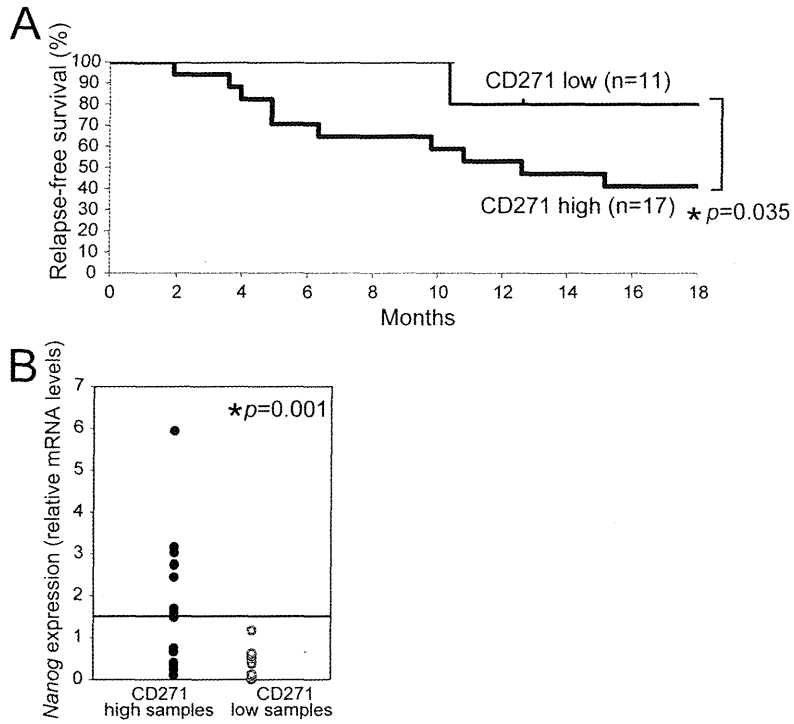

Figure 6. Gene expression of CD271 and Nanog in clinical specimens of HPC. (A) Kaplan-Meier analysis for the relapse-free survival rate according to the *CD271* mRNA level, in tumor tissues derived from 28 HPC patients by surgery. Real-time RT-PCR analyses were conducted, normalized to the expression of *GAPDH*, and the fold-change in *CD271* expression levels in the tumor versus normal mucosa was calculated. The cut-off value for the *CD271*-expression index was 1.5. *Statistically significant. (B) *Nanog* expression was examined by real-time RT-PCR. Cut-off value for the *Nanog* expression index was 1.5. *Statistically significant. Closed circles, CD271 high; open circles, CD271 low.
doi:10.1371/journal.pone.0062002.g006

study, the *Nanog* expression was elevated in the $CD271^+$ cells of all three HPC xenograft lines. Furthermore, all the *Nanog*-high cases also had *CD271*-high expression in our clinical specimens. Thus, we consider the $CD271^+$ cells in HPC to have pluripotent stemness characteristics with high *Nanog* expression.

Treatment resistance is a well-known characteristic of CSCs. For example, $CD133^+$ glioma stem cells show radioresistance [43], and $CD44^+CD24^-$ breast CSCs are chemoresistant [44]. These treatment resistances are considered to be associated with treatment failure, for instance with cancer relapse. In our study, the $CD271^+$ cells of HPC were at least partially CDDP-resistant as assessed by both IHC and FACS analyses. In esophageal SCC, Huang et al previously demonstrated a similar CDDP resistance of $CD271^+$ cells in vitro using ^{64}copper accumulation assays [16]. Our findings also suggested the involvement of the drug transporters ABCC2, ABCB5, and ABCG2 in the function of the $CD271^+$ cells. The elevated *ABCC2* expression may be responsible for the CDDP resistance of the $CD271^+$ cells [45]. The up-regulation of *ABCB5* and *ABCG2* may similarly confer multidrug resistance on $CD271^+$ cells. Interestingly, ABCB5 marks a putative cancer stem cell compartment in oral cancer [46], and cancer stem cells of the laryngeal cancer cell line Hep-2 show an increase in *ABCG2* expression [47]. Taken together, the up-regulation of ATP-binding transporters may contribute to the malignant phenotypes of $CD271^+$ cells. However, the differential drug resistance *in vivo* needs to be interpreted carefully, because additional factors, such as differential localization within a tumor and interaction with the stroma may affect cell survival. In the present study, treatment resistance was also indirectly supported by the clinical outcomes. Immunohistochemical and gene expression analyses for CD271 using primary HPC specimens indicated that high CD271 expression was correlated with a poor prognosis for the patient. Disease-specific survival analyses of 83 HPC cases, as well as the relapse-free survival, suggested that the CD271 expression determined by IHC staining was correlated with a poor prognosis and tumor aggressiveness. From these findings, we speculate that elevated CD271 expression is a good marker for a poor prognosis. Similarly, CD271 is reported to be a marker for poor prognosis in oral cancer [48]. Accordingly, we are in the process of setting up a larger clinico-pathological study to investigate whether CD271 can be a unique prognostic marker of HPC, when adjusting multiple parameters, such as clinical-, T- and N-stages. At present, with limited number of cases, both the disease-specific and relapse-free survival rates of CD271 high cases tend to be lower (e.g., Stage IV, 18-month relapse-free survival: CD271-low, 66.7% vs CD271-high, 18.2%, $p = 0.09$). By increasing the number of cases, we speculate that CD271 can be an independent prognostic marker of HPC in the future.

There are some limitations in our study. First, despite the enhanced tumor-initiating capability of the $CD271^+$ cells, the $CD271^-$ cells also initiated tumors, but with a longer latency and less efficiency. Furthermore, IHC and FACS analyses of the $CD271^-$derived tumors revealed that they included some $CD271^+$ cells (**Figure S6**). A certain level of plasticity may account for this inter-conversion. Alternatively, a minor contamination of the $CD271^-$ cells by $CD271^+$ cells during the sorting procedure

cannot be ruled out. Second, the subcutaneous xenografting experiment requires careful evaluation, as it may differ from orthotopic grafting. In addition, CD271-positivity detected by IHC and FACS may potentially include certain difference in the sensitivity, the dynamic range, and the specificity. Therefore, careful interpretation may be required upon comparison of the data obtained by these two methods.

Taken together, we conclude that the $CD271^+$ cells in human HPC possess tumor-initiating capability and some CSC-like characteristics. Our findings will help pave the way for the development of a novel strategy for treating HPC, using CD271, for future clinical interventions. Further study will be needed to investigate the function of CD271 in CSCs.

Supporting Information

Figure S1 Histology of xenotransplanted HPC tumors and their original primary samples. Primary HPC tumors obtained from three independent patients were transplanted into NOG mice, and the respective xenotransplanted tumors were dissected from the mice. Tissues of the primary HPC tumors and their xenotransplanted tumors were stained with hematoxylin and eosin (H&E). The primary and xenotransplanted tumors were histologically indistinguishable. Scale bar: 100 μm.
(TIF)

Figure S2 IHC of xenotransplanted HPC tumors for CD271 and CKs. IHC for CD271, CK5/6, and CK8 in serial sections of a xenograft tumor. IHC is performed as described in Materials and Methods S1. Immunopositivity appears brown. Scale bar: 100 μm.
(TIF)

Figure S3 IHC of xenotransplanted HPC tumors for Nanog and MMPs. IHC for CD271 and Nanog (A), and CD271 and MMPs (B) in serial sections of a xenograft tumor. IHC is performed as described in Materials and Methods S1. Immunopositivity appears brown. Scale bar: 100 μm.
(TIF)

Figure S4 Expression of Sox-2 and Oct-4 in $CD271^+$ and $CD271^-$ cells from HPC. *Sox-2* and *Oct-4* expression in the $CD271^+$ and $CD271^-$ cells was analyzed by real-time RT-PCR. Transcript levels were normalized to that of *GAPDH*, and the fold increase in the expression level in $CD271^+$ versus $CD271^-$ cells was calculated for each HPC line. Values are the mean±SD of triplicate experiments.
(TIF)

Figure S5 Expression of *MMP9*, *MMP11*, and *MT1-MMP* in the $CD271^+$ and $CD271^-$ cells of HPC. The *MMP9*, *MMP11*, and *MT1-MMP* expressions in $CD271^+$ and $CD271^-$ cells were analyzed by real-time RT-PCR. The transcript levels were normalized to that of *GAPDH*, and the fold change in *MMP9*, *MMP11* and *MT1-MMP* expression levels in $CD271^+$ versus $CD271^-$ cells was calculated for each sample. Values are the mean±SD of triplicate experiments.
(TIF)

Figure S6 Plasticity between the $CD271^-$ and $CD271^+$ populations. Tumors generated from $CD271^-$ cells, and $CD271^+$ cells were analyzed by IHC and FACS for CD271. Immunopositivity appears brown. Scale bar: 100 μm.
(TIF)

Table S1 Primer Sequence.
(DOCX)

Table S2 Short summary of HPC xenograft lines.
(DOCX)

Table S3 Correlation between CD271 expression in IHC and characteristics of HPC patients.
(DOCX)

Table S4 Correlation between CD271 expression and clinical characteristics of HPC patients.
(DOCX)

Table S5 Tumorigenicity of $CD44^+$ and $CD44^-$ cells in vivo (HPCM1). *In vivo* tumorigenesis assay is performed as described in Materials and Methods S1.
(DOCX)

Materials and Methods S1.
(DOCX)

Acknowledgments

The authors thank Ms. Kuniko Komuro for her assistance with the clinical sample preparations. This study was partly supported by Biomedical Research Core of Tohoku University School of Medicine.

Author Contributions

Conceived and designed the experiments: TI KS NT. Performed the experiments: TI SO KO. Analyzed the data: TI KT KY IS K. Satoh KM SS. Wrote the paper: TI K. Sugamura NT.

References

1. Parkin DM, Bray F, Ferlay J, Pisani P (2005) Global cancer statistics, 2002. CA Cancer J Clin 55: 74–108.
2. Day GL, Blot WJ, Shore RE, McLaughlin JK, Austin DF, et al. (1994) Second cancers following oral and pharyngeal cancers: role of tobacco and alcohol. J Natl Cancer Inst 86: 131–137.
3. Spector JG, Sessions DG, Haughey BH, Chao KS, Simpson J, et al. (2001) Delayed regional metastases, distant metastases, and second primary malignancies in squamous cell carcinomas of the larynx and hypopharynx. Laryngoscope 111: 1079–1087.
4. Berrino F, Gatta G (1998) Variation in survival of patients with head and neck cancer in Europe by the site of origin of the tumours. EUROCARE Working Group. Eur J Cancer 34: 2154–2161.
5. Dick JE (2008) Stem cell concepts renew cancer research. Blood 112: 4793–4807.
6. Clarke MF, Dick JE, Dirks PB, Eaves CJ, Jamieson CH, et al. (2006) Cancer stem cells–perspectives on current status and future directions: AACR Workshop on cancer stem cells. Cancer Res 66: 9339–9344.
7. Prince ME, Sivanandan R, Kaczorowski A, Wolf GT, Kaplan MJ, et al. (2007) Identification of a subpopulation of cells with cancer stem cell properties in head and neck squamous cell carcinoma. Proc Natl Acad Sci U S A 104: 973–978.
8. Oh SY, Kang HJ, Kim YS, Kim H, Lim YC (2012) CD44-negative cells in head and neck squamous carcinoma also have stem-cell like traits. Eur J Cancer.
9. Coulon A, Flahaut M, Muhlethaler-Mottet A, Meier R, Liberman J, et al. (2011) Functional sphere profiling reveals the complexity of neuroblastoma tumor-initiating cell model. Neoplasia 13: 991–1004.
10. Bibel M, Barde YA (2000) Neurotrophins: key regulators of cell fate and cell shape in the vertebrate nervous system. Genes Dev 14: 2919–2937.
11. Nakamura T, Endo K, Kinoshita S (2007) Identification of human oral keratinocyte stem/progenitor cells by neurotrophin receptor p75 and the role of neurotrophin/p75 signaling. Stem Cells 25: 628–638.
12. Li X, Shen Y, Di B, Li J, Geng J, et al. (2012) Biological and clinical significance of p75NTR expression in laryngeal squamous epithelia and laryngocarcinoma. Acta Otolaryngol 132: 314–324.
13. Okumura T, Shimada Y, Imamura M, Yasumoto S (2003) Neurotrophin receptor p75(NTR) characterizes human esophageal keratinocyte stem cells in vitro. Oncogene 22: 4017–4026.
14. Civenni G, Walter A, Kobert N, Mihic-Probst D, Zipser M, et al. (2011) Human CD271-positive melanoma stem cells associated with metastasis establish tumor heterogeneity and long-term growth. Cancer Res 71: 3098–3109.

15. Boiko AD, Razorenova OV, van de Rijn M, Swetter SM, Johnson DL, et al. (2010) Human melanoma-initiating cells express neural crest nerve growth factor receptor CD271. Nature 466: 133–137.
16. Huang SD, Yuan Y, Liu XH, Gong DJ, Bai CG, et al. (2009) Self-renewal and chemotherapy resistance of p75NTR positive cells in esophageal squamous cell carcinomas. BMC Cancer 9: 9.
17. Chaubal S, Wollenberg B, Kastenbauer E, Zeidler R (1999) Ep-CAM–a marker for the detection of disseminated tumor cells in patients suffering from SCCHN. Anticancer Res 19: 2237–2242.
18. Lim YC, Oh SY, Cha YY, Kim SH, Jin X, et al. (2011) Cancer stem cell traits in squamospheres derived from primary head and neck squamous cell carcinomas. Oral Oncol 47: 83–91.
19. de Jonge-Peeters SD, Kuipers F, de Vries EG, Vellenga E (2007) ABC transporter expression in hematopoietic stem cells and the role in AML drug resistance. Crit Rev Oncol Hematol 62: 214–226.
20. Lapidot T, Sirard C, Vormoor J, Murdoch B, Hoang T, et al. (1994) A cell initiating human acute myeloid leukaemia after transplantation into SCID mice. Nature 367: 645–648.
21. Clevers H (2011) The cancer stem cell: premises, promises and challenges. Nat Med 17: 313–319.
22. Al-Hajj M, Wicha MS, Benito-Hernandez A, Morrison SJ, Clarke MF (2003) Prospective identification of tumorigenic breast cancer cells. Proc Natl Acad Sci U S A 100: 3983–3988.
23. Clay MR, Tabor M, Owen JH, Carey TE, Bradford CR, et al. (2010) Single-marker identification of head and neck squamous cell carcinoma cancer stem cells with aldehyde dehydrogenase. Head Neck 32: 1195–1201.
24. Wei XD, Zhou L, Cheng L, Tian J, Jiang JJ, et al. (2009) In vivo investigation of CD133 as a putative marker of cancer stem cells in Hep-2 cell line. Head Neck 31: 94–101.
25. Li C, Heidt DG, Dalerba P, Burant CF, Zhang L, et al. (2007) Identification of pancreatic cancer stem cells. Cancer Res 67: 1030–1037.
26. Zhang S, Balch C, Chan MW, Lai HC, Matei D, et al. (2008) Identification and characterization of ovarian cancer-initiating cells from primary human tumors. Cancer Res 68: 4311–4320.
27. Nakshatri H, Srour EF, Badve S (2009) Breast cancer stem cells and intrinsic subtypes: controversies rage on. Curr Stem Cell Res Ther 4: 50–60.
28. Ritchie KE, Nor JE (2012) Perivascular stem cell niche in head and neck cancer. Cancer Lett.
29. Morrison SJ, Spradling AC (2008) Stem cells and niches: mechanisms that promote stem cell maintenance throughout life. Cell 132: 598–611.
30. Krishnamurthy S, Dong Z, Vodopyanov D, Imai A, Helman JI, et al. (2010) Endothelial cell-initiated signaling promotes the survival and self-renewal of cancer stem cells. Cancer Res 70: 9969–9978.
31. Liotta LA, Kohn EC (2001) The microenvironment of the tumour-host interface. Nature 411: 375–379.
32. Bankfalvi A, Piffko J (2000) Prognostic and predictive factors in oral cancer: the role of the invasive tumour front. J Oral Pathol Med 29: 291–298.
33. Bryne M, Boysen M, Alfsen CG, Abeler VM, Sudbo J, et al. (1998) The invasive front of carcinomas. The most important area for tumour prognosis? Anticancer Res 18: 4757–4764.
34. Rosenthal EL, Matrisian LM (2006) Matrix metalloproteases in head and neck cancer. Head Neck 28: 639–648.
35. Pullen NA, Anand M, Cooper PS, Fillmore HL (2012) Matrix metalloproteinase-1 expression enhances tumorigenicity as well as tumor-related angiogenesis and is inversely associated with TIMP-4 expression in a model of glioblastoma. J Neurooncol 106: 461–471.
36. Justilien V, Regala RP, Tseng IC, Walsh MP, Batra J, et al. (2012) Matrix metalloproteinase-10 is required for lung cancer stem cell maintenance, tumor initiation and metastatic potential. PLoS One 7: e35040.
37. Mitsui K, Tokuzawa Y, Itoh H, Segawa K, Murakami M, et al. (2003) The homeoprotein Nanog is required for maintenance of pluripotency in mouse epiblast and ES cells. Cell 113: 631–642.
38. Chambers I, Colby D, Robertson M, Nichols J, Lee S, et al. (2003) Functional expression cloning of Nanog, a pluripotency sustaining factor in embryonic stem cells. Cell 113: 643–655.
39. Zhang J, Espinoza LA, Kinders RJ, Lawrence SM, Pfister TD, et al. (2012) NANOG modulates stemness in human colorectal cancer. Oncogene.
40. Jeter CR, Liu B, Liu X, Chen X, Liu C, et al. (2011) NANOG promotes cancer stem cell characteristics and prostate cancer resistance to androgen deprivation. Oncogene 30: 3833–3845.
41. Jeter CR, Badeaux M, Choy G, Chandra D, Patrawala L, et al. (2009) Functional evidence that the self-renewal gene NANOG regulates human tumor development. Stem Cells 27: 993–1005.
42. Chiou SH, Yu CC, Huang CY, Lin SC, Liu CJ, et al. (2008) Positive correlations of Oct-4 and Nanog in oral cancer stem-like cells and high-grade oral squamous cell carcinoma. Clin Cancer Res 14: 4085–4095.
43. Bao S, Wu Q, McLendon RE, Hao Y, Shi Q, et al. (2006) Glioma stem cells promote radioresistance by preferential activation of the DNA damage response. Nature 444: 756–760.
44. Li X, Lewis MT, Huang J, Gutierrez C, Osborne CK, et al. (2008) Intrinsic resistance of tumorigenic breast cancer cells to chemotherapy. J Natl Cancer Inst 100: 672–679.
45. Galluzzi L, Senovilla L, Vitale I, Michels J, Martins I, et al. (2012) Molecular mechanisms of cisplatin resistance. Oncogene 31: 1869–1883.
46. Grimm M, Krimmel M, Polligkeit J, Alexander D, Munz A, et al. (2012) ABCB5 expression and cancer stem cell hypothesis in oral squamous cell carcinoma. Eur J Cancer 48: 3186–3197.
47. Yang JP, Liu Y, Zhong W, Yu D, Wen LJ, et al. (2011) Chemoresistance of CD133+ cancer stem cells in laryngeal carcinoma. Chin Med J (Engl) 124: 1055–1060.
48. Soland TM, Brusevold IJ, Koppang HS, Schenck K, Bryne M (2008) Nerve growth factor receptor (p75 NTR) and pattern of invasion predict poor prognosis in oral squamous cell carcinoma. Histopathology 53: 62–72.

J Gastroenterol
DOI 10.1007/s00535-012-0596-x

ORIGINAL ARTICLE—LIVER, PANCREAS, AND BILIARY TRACT

Sequential immunological analysis of HBV/HCV co-infected patients during Peg-IFN/RBV therapy

Yasuteru Kondo · Yoshiyuki Ueno · Masashi Ninomiya · Keiichi Tamai · Yasuhito Tanaka · Jun Inoue · Eiji Kakazu · Koju Kobayashi · Osamu Kimura · Masahito Miura · Takeshi Yamamoto · Tomoo Kobayashi · Takehiko Igarashi · Tooru Shimosegawa

Received: 29 August 2011 / Accepted: 28 March 2012

Abstract

Background The immunopathogenesis of dual chronic infection with hepatitis B virus and hepatitis C virus (HBV/HCV) remains unclear. The in vivo suppressive effects of each virus on the other have been reported. In this study we aimed to analyze the virological and immunological parameters of HBV/HCV coinfected patients during pegylated interferon/ribavirin (Peg-IFN/RBV) therapy.

Methods One patient with high HBV-DNA and high HCV-RNA titers (HBV-high/HCV-high) and 5 patients with low HBV-DNA and high HCV-RNA titers (HBV-low/HCV-high) were enrolled. Twenty patients monoinfected with HBV and 10 patients monoinfected with HCV were enrolled as control subjects.. In vitro cultures of Huh 7 cells with HBV/HCV dual infection were used to analyze the direct interaction of HBV/HCV.

Results Direct interaction of HBV clones and HCV could not be detected in the Huh-7 cells. In the HBV-high/HCV-high-patient, the HCV-RNA level gradually declined and HBV-DNA gradually increased during Peg-IFN/RBV therapy. Activated CD4- and CD8-positive T cells were increased at 1 month of Peg-IFN/RBV-therapy, but HBV-specific IFN-γ-secreting cells were not increased and HBV-specific interleukin (IL)-10 secreting cells were increased. The level of HBV- and HCV-specific IFN-γ-secreting cells in the HBV-high/HCV-high-patient was low in comparison to that in the HBV- or HCV-monoinfected patients. In the HBV-low/HCV-high-patient, HCV-RNA and HBV-DNA rapidly declined during Peg-IFN/RBV therapy. Activated CD4- and CD8-positive T cells were increased, and HBV- and HCV-specific IFN-γ-secreting cells were also increased during Peg-IFN/RBV-therapy.

Conclusion The immunological responses of the HBV-high/HCV-high patient were low in comparison to the responses in HBV and HCV monoinfected patients. Moreover, the response of immune cells in the HBV-high/HCV-high patient during Peg-IFN/RBV therapy was insufficient to suppress HBV and HCV.

Keywords Dual infection · HBV · HCV · Immunopathogenesis

Electronic supplementary material The online version of this article (doi:10.1007/s00535-012-0596-x) contains supplementary material, which is available to authorized users.

Y. Kondo · Y. Ueno (✉) · M. Ninomiya · K. Tamai · J. Inoue · E. Kakazu · O. Kimura · T. Shimosegawa
Division of Gastroenterology, Tohoku University Graduate School of Medicine, 1-1 Seiryo, Aobaku, Sendai, Miyagi, Japan
e-mail: y-ueno@med.id.yamagata-u.ac.jp; yeuno@med.tohoku.ac.jp

Y. Tanaka
Virology and Liver Unit, Nagoya City University Medical School, Nagoya, Japan

K. Kobayashi
Tohoku University Graduate School of Medicine, 2-1 Seiryo, Aobaku, Sendai, Miyagi, Japan

M. Miura
Department of Gastroenterology, South Miyagi Medical Center, Oogawara, Miyagi, Japan

T. Yamamoto
Department of Gastroenterology, Tohoku Kosei-Nenkin Hospital, Sendai, Miyagi, Japan

T. Kobayashi
Department of Hepatology, Tohoku Rosai Hospital, Sendai, Miyagi, Japan

T. Igarashi
Department of Gastroenterology, Osaki Citizen Hospital, Osaki, Japan

Published online: 16 May 2012

Introduction

Hepatitis B virus (HBV) and Hepatitis C virus (HCV) are noncytopathic viruses that cause chronic hepatitis and hepatocellular carcinoma (HCC) [1, 2]. HBV now affects more than 400 million people worldwide, and persistent infection develops in ~5 % of adults and 95 % of neonates who become infected with HBV [3]. HCV infects about 170 million people worldwide and is a major cause of chronic hepatitis, cirrhosis, and HCC [4]. Some groups have mentioned that dual infection with HBV/HCV is not uncommon in Asian patients [5, 6]. The prevalence of patients with dual HBV/HCV infection is approximately 10–15 %, although it likely differs among countries [7–9]. Co-infection with HBV/HCV has been associated with severe liver disease and frequent progression to cirrhosis [10]. Moreover, a significantly higher incidence of HCC and liver-related mortality was noted in patients with HBV/HCV co-infection [11, 12]. However, some groups reported, based on a meta-analysis, that dual infection with HBV/HCV did not increase the risk of HCC [13, 14]. These contradictory reports could be explained by the rarity of dual infection with HBV/HCV in patients without clinically evident liver disease. It might be difficult to estimate the hepatocarcinogenic risk of dual infection compared with that of either infection alone in such clinical settings [15].

An inverse relationship in the replicative levels of the two viruses has been noted, suggesting direct or indirect effects in vivo [16]. More recently, some groups have reported, using an in vitro infection system, that there is little direct interaction of HBV/HCV in coinfected hepatocytes [17, 18]. Therefore, the viral interference observed in coinfected patients is probably due to indirect mechanisms mediated by the innate and/or adaptive host immune responses.

The cellular immune response to HBV and HCV plays an important role in the pathogenesis of chronic hepatitis, cirrhosis, and HCC [19–21]. Hyporesponsiveness of HBV- or HCV-specific T-helper 1 cells and excessive regulatory function of $CD4^+CD25^+FoxP3^+$ regulatory T cells (Tregs) in peripheral blood have been shown in patients with chronic hepatitis B and C [22–34]. Recently, we reported that HBV replication stress could enhance the suppressive activity of Tregs via TLR2 [35]. However, little is known about the immunopathogenesis of HBV/HCV dual infection.

Dual infection can be classified into several groups (e.g., group A: HBV active and HCV active; group B: HBV inactive and HCV active; and group C: HBV active and HCV inactive) [36]. HCV is reported to be the dominant virus in HBV/HCV dual infection, but the dominance of either virus might be due to the genotypes of each virus and/or ethnic differences that could affect the proliferative activity of the viruses [36]. In this study, we investigated immunopathogenesis in a group A patient and in group B patients during therapy with pegylated interferon-α2b (Peg-IFN-α2b) plus ribavirin.

Patients, materials, and methods

Patients

One patient with high HBV-DNA and high HCV-RNA titers (HBV-high/HCV-high; patient A) and 5 patients with low HBV-DNA and high HCV-RNA titers (HBV-low/HCV-high) were enrolled (one of these patients, whose results were analyzed in detail, was termed patient B; see findings below in the "Results"). Twenty patients monoinfected with HBV and 10 patients monoinfected with HCV were enrolled as control subjects. None of the patients had liver disease due to other causes, such as alcohol, drugs, congestive heart failure, or autoimmune diseases. Permission for the study was obtained from the Ethics Committee at Tohoku University Graduate School of Medicine (permission no. 2006-194). Written informed consent was obtained from all the participants enrolled in this study. Participants were monitored for two years. At each assessment, patients were evaluated by biochemical laboratory tests, immunological analysis, and virological tests. Liver histology was analyzed at the start of Peg-IFN/RBV therapy by using laparoscopic liver biopsy samples and by employment of the METAVIR score.

Detection of interleukin (IL)-28B polymorphism

Genomic DNA was isolated from peripheral blood mononuclear cells (PBMCs) using an automated DNA isolation kit. Then polymorphism of IL-28B (rs8099917) was analyzed using real-time polymerase chain reaction (PCR) (TaqMan SNP Genotyping Assay, Applied Biosystems, CA, USA). Detection of the IL-28B polymorphism was approved by the Ethics Committee at Tohoku University Graduate School of Medicine (permission no. 2010-323).

Isolation of peripheral blood mononuclear cells (PBMCs) and flow cytometry

Peripheral blood mononuclear cells (PBMCs) were isolated from fresh heparinized blood by means of Ficoll-Hypaque density gradient centrifugation (Amersham Bioscience, Uppsala, Sweden). PBMCs were stained with CD3, CD4, CD8, CD19, CD25, CD40, CD56, CD86, HLA-DR, NKG2D, and isotype control antibodies (Becton Dickinson, NJ, USA) for 15 min on ice to analyze the frequency

of $CD3^+CD4^+$HLA-DR^+ cells, $CD3^+CD8^+$HLA-DR^+cells, $CD4^+CD25^+$ Tregs, $CD3^-CD16^-CD56^{high}$natural killer (NK) cells, and $CD3^-CD16^+CD56^{dim}$ NK cells. The frequencies of the immune subsets were analyzed by flow cytometry using FACS Canto-II (Becton Dickinson, NJ, USA).

ELISPOT assay

The detection of IFN-γ and IL-10 was performed using an ELISPOT Set (BD Biosciences, San Jose, CA, USA) according to the manufacturer's instructions. Cultures of PBMCs were established in triplicate on round-bottomed 96-well plates for all time points investigated, at a concentration of 3×10^5 cells per well in 100 µl RPMI 1640 containing 10 % fetal bovine serum (FBS). Positive spots were detected using an automated counting machine.

Detection of HBV-DNA and determination of HBV genotype

DNA was extracted from 100 µl of serum using SMITEST EX-R&D (Medical & Biological Laboratories, Nagoya, Japan) and dissolved in 20 µl of nuclease-free distilled water. The DNA preparation thus obtained (10 µl) was subjected to nested PCR with primers targeting the S gene of the HBV-DNA, as described previously [37]. Briefly, first-round PCR was carried out for 35 cycles (98 °C for 10 s, 55 °C for 15 s, and 72 °C for 1 min, with an additional 7 min in the last cycle) in the presence of PrimeSTAR HS DNA Polymerase (TaKaRa Bio, Shiga, Japan) and primers HB095 (sense, 5′-GAG TCT AGA CTC GTG GTG GAC-3′) and HB184 (antisense, 5′-CGA ACC ACT GAA CAA ATG GCA CCG-3′), for 25 cycles. This was followed by a second-round PCR consisting of 25 cycles using the same conditions as in the first round, with primers HB097 (sense, 5′-GAC TCG TGG TGG ACT TCT CTC-3′) and S2-2 (antisense, 5′-GGC ACT AGT AAA CTG AGC CA-3′). The HBV genotype was determined by phylogenetic analysis of the S gene sequence (437 nt) of the HBV isolates.

Detection of HCV RNA

RNAs were extracted from 250 µl of serum using TRIzol LS (Invitrogen, Tokyo, Japan). They were divided into two aliquots and each was assayed by reverse transcription (RT)-PCR with nested primers derived from the core region and NS5A interferon sensitivity determining region (ISDR) of the HCV genome. Nested PCR of the core region of the HCV genome was carried out with primers C008 (sense, 5′-AAC CTC AAA GAA AAA CCA AAC G-3′) and C011 (antisense, 5′-CAT GGG GTA CAT YCC GCT YG-3′) in the first round and C009 (sense, 5′-CCA CAG GAC GTY AAG TTC CC-3′) and C010 (antisense, 5′-AGG GTA TCG ATG ACC TTA CC-3′) in the second round. Nested primers that were derived from NS5A-ISDR of the HCV genomes were designed to amplify a 188-bp product with C004 (sense, 5′-ATG CCC ATG CCA GGT TCC AG-3′) and C005 (antisense, 5′-AGC TCC GCC AAG GCA GAA GA-3′) in the first round, and C006 (sense, 5′-ACC GG A TGT GGC AGT GCT CA-3′) and C007 (antisense, 5′-GTA ATC CGG GCG TGC CCA TA-3′) in the second round.

Analysis of nucleotide and amino acid sequences

The PCR products were sequenced directly on both strands using a BigDye Terminator version 3.1 Cycle Sequencing Kit on an ABI PRISM 3100 Genetic Analyzer (Applied Biosystems, Foster City, CA, USA). Sequence analysis was performed using Genetyx-Mac ver. 12.2.6 (Genetyx, Tokyo, Japan) and ODEN (version 1.1.1) from the DNA Data Bank of Japan (National Institute of Genetics, Mishima, Japan) [38]. Sequence alignments were generated using CLUSTAL W (Version 1.8) [39]. The phylogenetic tree was constructed by the neighbor-joining method [40]. The reliability of the phylogenetic results was assessed using 1000 bootstrap replicants [41]. The final tree was obtained with the Njplot program (version 2.2) [42].

Plasmid construction

HBV expression plasmids were constructed by previously published methods. Serum samples were obtained from two patients infected with HBV genotype Bj and two patients infected with HBV genotype C. HBV-DNA was extracted from 100 µl serum using a QIAamp DNA blood kit (QIAGEN, Hilden, Germany). Four primer sets were designed to amplify two fragments covering the entire HBV genome. Amplified fragments were inserted into a pGEM-T Easy Vector (Promega, Madison, WI, USA) and cloned in DH5a competent cells (TOYOBO, Osaka, Japan). Briefly, at least 5 clones of each fragment were sequenced and the consensus sequence was identified and used as a template for 1.24-fold the HBV genome of different genotypes (B1 indicates the genotype Bj35 clone; B2 indicates the genotype Bj56 clone; C1 indicates the genotype C-AT clone; and C2 indicates the genotype C-22 clone). The HCV-JFH-1 strain was provided by Dr. T. Wakita (National Institute of Infectious Diseases, Japan).

HCV and HBV expression in Huh 7 cells

Cell-culture-derived infectious HCV was generated as described previously [43]. The HCV was quantified as

follows: RNA was extracted from the Huh-7 culture supernatant using a QIAamp Viral RNA Kit (Qiagen, Valencia, CA, USA). The HCV RNA was quantified by real-time RT-PCR, using TaqMan EZ RT-PCR Core Reagents (Applied Biosystems) according to the manufacturer's protocol, using the published primers and probe [44]. The filtered (0.45 μm) culture supernatant of HCV-infected Huh-7 cells containing 2×10^8 HCV RNA copies/ml [equivalent to 9.7×10^4 focus-forming units (ffu)/ml] was used for the experiments. To analyze HCV-RNA in the supernatant, Huh-7 cells (2×10^5 cells in a 6-well plate) were infected with JFH-1 (multiplicity of infection [MOI] = 0.01) and after 4 h the cells were washed twice with phosphate-buffered saline (PBS). The supernatants were then collected and the cells were reseeded at 2×10^5 cells per 6-well plate. Then the HBV expression and mock plasmid were transfected by FuGENE6 (Roche Applied Science, IN, USA). The supernatant of the culture medium was collected 72 h after transfection. Quantification of HBV-DNA and HCV-RNA was carried out using real-time PCR.

IFN-α was added 24 h after the transfection of the HBV plasmids, and the supernatant of the culture medium was then collected 48 h after the addition of the IFN-α.

Results

Clinical characteristics of patients A and B

Patient A (high HBV-DNA titer and high HCV-RNA titer)

Patient A was a 44 year-old man with a high aspartate aminotransferase/alanine aminotransferase (AST/ALT) level. The prothrombin time-international normalized ratio (PT-INR) was in the normal range. Patient A had high HBV-DNA titers and high HCV-RNA titers (Table 1). His liver histology was classified as A2/F3 (Fig. 1). The laparoscopic analysis indicated moderate inflammation and intermediate fibrosis. The liver surfaces of the right lobe and left lobe were almost the same phenotype. Polymorphism of IL-28B (rs8099917) was T/G (hetero allele).

Patient B (low HBV-DNA titer and high HCV-RNA titer)

Patient B was a 63 year-old man with a low AST/ALT level. PT-INR was in the normal range. Patient B had low HBV-DNA titers and high HCV-RNA titers. The liver histology was classified as A2/F1 (Fig. 1). The liver surface showed moderate inflammation and was smooth. The polymorphism of IL-28B (rs8099917) was T/T (major homo allele).

Biopsy samples from patients with dual HBV and HCV infection were collected at the main liver centers in Miyagi prefecture. Fifteen HBV/HCV dual-infected patients were found in this study (Supplementary Table 1). Many of these patients had HCV-dominant infection and undetectable levels of HBV replication (10/15 patients). Most of the patients were HB envelope antigen (eAg)-negative and HBe antibody (Ab)-positive (14/14 patients). All HBV/HCV dual-infected patients who had received Peg-IFN-based

Table 1 Background of HBV/HCV dual-infected patients

	Patient A HCV high titer/ HBV high titer	Patient B HCV high titer/ HBV low titer	Normal range
Gender	Male	Male	
Age (years)	44	63	
HCV-RNA	6.5	5.5	log copies/ml
HCV genotype	1b	1b	
HBV-DNA	5.5	3.5	log copies/ml
HBV genotype	C	Bj	
HBe-Ag	129.5	0.5	0–0.9 index
HBe-Ab	0.1	99.3	0–49 %
Total bilirubin	0.7	1.2	0.2–1.2 mg/dl
Direct bilirubin	0.1	0.1	0–0.3 mg/dl
γ-GTP	208	31	8–57 IU/l
AST	138	33	12–30 IU/l
ALT	256	38	8–35 IU/l
Hb-A1c	5.3	5.4	4.3–5.8 %
Glu	103	83	68–106 mg/dl
BMI	25.34	18.75	
T-cho	160	195	128–220 mg/dl
LDL-cho	69	93	70–139 mg/dl
HDL-cho	37	67	36–89 md/dl
WBC	7800	5100	3200–9600/μl
RBC	491	446	428–566 × 10^4/μl
Hb	17.1	14.1	13.6–17.4 g/dl
PLT	169000	176000	155000–347000/μl
PT-INR	0.87	0.96	0–1.15 INR
Liver histology	A2/F3	A2/F1	METAVIR score
IL-28B SNP (rs8099917)	T/G	T/T	

HCV hepatitis C virus, *HBV* hepatitis B virus, e-*Ag* envelope antigen, *e-Ab* envelope antibody, *γ-GTP* γ-guanosine triphosphate, *AST* aspartate aminotransferase, *ALT* alanine aminotransferase, *Hb* hemoglobin, *Glu* glucose, *BMI* body mass index, *T-cho* total cholesterol, *LDL* low-density lipoprotein, *HDL* high-density lipoprotein, *PLT* platelets, *PT-INR* prothromin time-international normalized ratio, *IL* interleukin, *SNP* single-nucleotide polymorphism

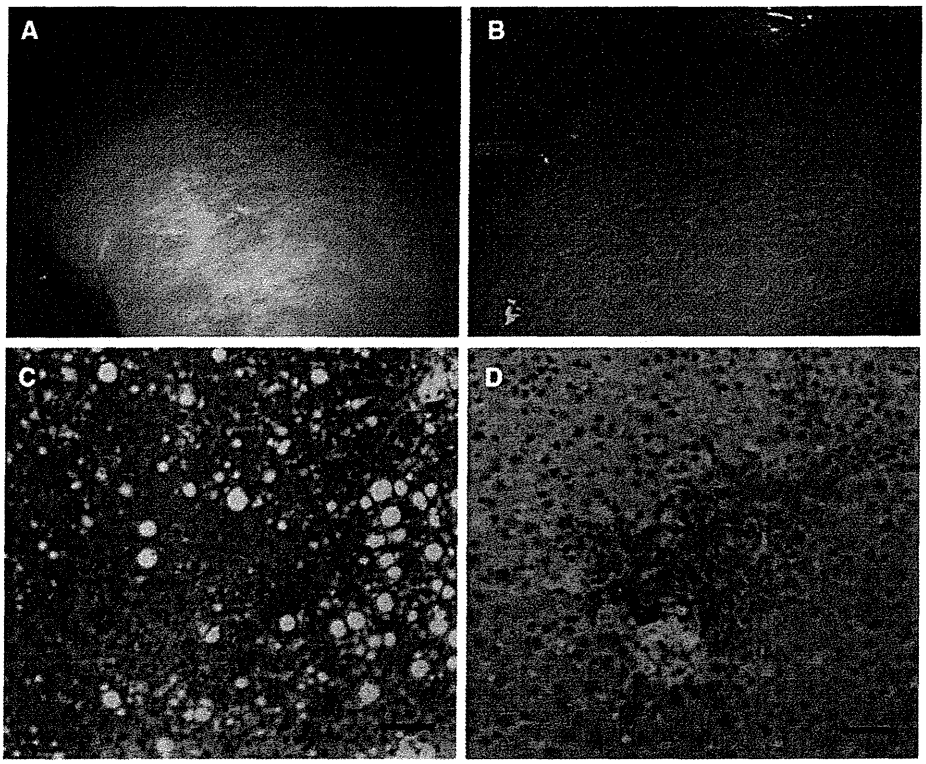

Fig. 1 Laparoscopic liver biopsy. The laparoscopic images of the liver surfaces of patient A (**a**) and patient B (**b**) are shown. Histopathology of patient A (**c**) and patient B (**d**) is also shown. *Bars* = 50 μm

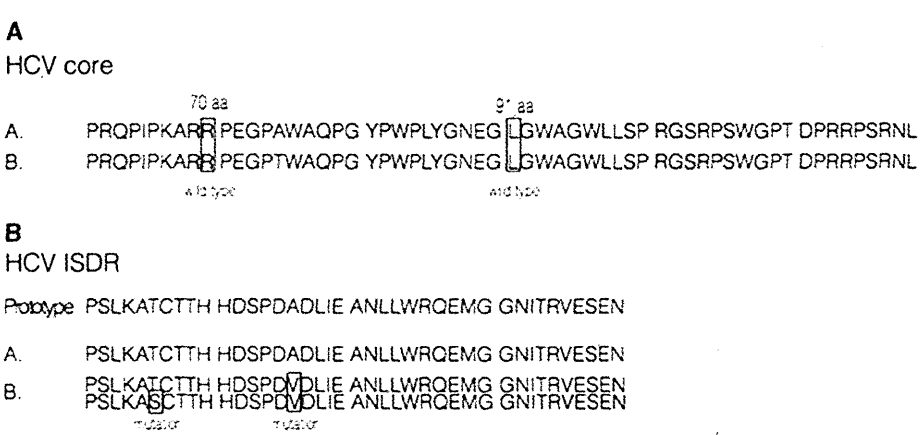

Fig. 2 Virological analysis of hepatitis B virus (HBV) and hepatitis C virus (HCV) in HBV/HCV dual infection. The amino acid sequences of the HCV-core region including core-70 and core-91, which were previously reported as determinants of the sensitivity to pegylated interferon/ribavirin (Peg-IFN/RBV) therapy, in patient A and patient B are shown (**a**). The amino acid sequences of the interferon sensitivity determining region (*ISDR*), which were previously reported as determinants of the sensitivity to IFN, in patients A and B are shown (**b**)

treatment achieved a sustained viral response (SVR) (5/5 patients). These data indicated that HCV-dominant dual-infected patients had good responses to treatment for HCV infection.

Virological analysis of HBV/HCV in patients A and B

The HCV genotype in both patient A and patient B was 1b. The sequences of amino acids in the ISDR region and HCV

core-70 and core-91 amino acids were analyzed by direct sequencing. Both patients had wild-type core-70 and core-91 amino acids (Fig. 2a). None of the mutations of the ISDR region was detected in patient A, but two of the mutations of the ISDR region were detected in patient B (Fig. 2b). The genotypes of HBV in patients A and B were analyzed by direct sequencing and phylogenetic tree analysis. The genotype of HBV in patient A was genotype C, which has been reported as difficult-to-treat HBV. The genotype of HBV in patient B was genotype Bj, which has been reported as easy-to-treat HBV in comparison to genotype C [45–47].

Sequential analysis of biochemical and virological data during Peg-IFN/RBV therapy

Patient A

In patient A, HCV-RNA gradually declined during Peg-IFN/RBV therapy. On the other hand, the HBV-DNA gradually increased during Peg-IFN/RBV therapy (Fig. 3a). The amount of HBeAg started to increase 9 months after the start of Peg-IFN/RBV therapy. HCV-RNA started to increase 12 months after the start of Peg-IFN/RBV therapy, although Peg-IFN/RBV was still being administered up to 18 months after the start of Peg-IFN/RBV therapy (Fig. 3a).

Patient B

In patient B, HCV-RNA and HBV-DNA rapidly declined after the start of Peg-IFN/RBV therapy (Fig. 3b). HCV-RNA could not be detected in peripheral blood 2 months after the start of Peg-IFN/RBV therapy. Peg-IFN/RBV was administered up to 12 months after the start of the Peg-IFN/RBV therapy. The amounts of HBeAb and HBeAg did not change during the Peg-IFN/RBV therapy (Fig. 3b).

Sequential immunological analysis during Peg-IFN/RBV therapy

We analyzed various subsets of immune cells that could affect the immunopathogenesis of HBV/HCV dual infection. NK cells ($CD3^-CD16^-CD56^{high}$ and $CD3^-CD16^+CD56^{dim}$) and NK-T cells ($CD3^+CD56^+CD16^+$, $CD3^+CD56^+CD16^-$ and $CD3^+CD56^-CD16^+$) were analyzed (Supplementary Fig. 1A). The $CD3^-$ gated lymphocytes were separated into 4 groups (a, b, c, and d). For these subsets, (a) indicated the presence of $CD3^-CD16^-CD56^{high}$ NK cells that could produce various cytokines vigorously and had low cytotoxic activity. Subset (b) showed $CD3^-CD16^+CD56^{dim}$ NK cells that had weak cytokine production ability and high cytotoxic activity.

The $CD3^+$ gated lymphocytes were separated into 3 groups (a, b, and c). The activated $CD3^+$, $CD3^+CD4^+$, and $CD3^+CD8^+$ T cells were analyzed (Supplementary Fig. 1B). HLA-DR^+ activated $CD3^+$, $CD3^+CD4^+$, and $CD3^+CD8^+$ T cells could be clearly distinguished by FACS analysis. Additionally, representative dot plots of Tregs and B cells were created (shown in Supplementary Fig. 1C). The frequencies of $CD3^-CD16^+CD56^{dim}$ NK cells, $CD3^+CD16^-CD56^+$ NK-T cells, activated $CD3^+CD4^+$ T cells, and activated $CD3^+CD8^+$ T cells fluctuated similarly during Peg-IFN/RBV therapy in patient A (Supplementary Fig. 1D). Activated T cells were increased at one month of Peg-IFN/RBV therapy, and the above subsets of lymphocytes gradually decreased up to 3 months of Peg-IFN/RBV therapy. After that, these cells gradually increased again up to 9 months of Peg-IFN/RBV therapy. In patient A, after 9 months of Peg-IFN/RBV therapy, these cells had decreased again (Supplementary Fig. 1D). The frequency of Tregs and activated B cells (data not shown) did not change during Peg-IFN/RBV therapy in patient A (Supplementary Fig. 1D). On the other hand, in patient B, the frequencies of $CD3^-CD16^+CD56^{dim}$ NK cells, $CD3^+CD16^-CD56^+$ NK-T cells, activated $CD3^+CD4^+$ T cells, and activated $CD3^+CD8^+$ T cells were increased and sustained during Peg-IFN/RBV therapy (Supplementary Fig. 1E). Five HCV monoinfected patients were analyzed by the same protocol (Supplementary Fig 1F). The mean frequency of various kinds of immune subsets was analyzed (Supplementary Fig 1F). The tendency of immunological reactions during Peg-IFN/RBV therapy in these five patients was similar to that in patient B.

Analysis of HBV- and HCV-specific immune responses

The analysis of HBV- and HCV-specific-immune responses was carried out by ELISPOT assay. Representative spots of IFN-γ are shown in Fig. 4a. In patient A, HCV- and HBV-specific IFN-γ secretion activities were remarkably low in comparison to the IL-10 secretion activity. Moreover, in patient A, the induction of IFN-γ-secreting cells could not be detected after Peg-IFN/RBV therapy, especially in regard to HBV-core specific IFN-γ secretion in PBMCs (Fig. 4b). On the other hand, in patient B, the HBV-core specific IFN-γ-secreting cells were high in comparison to those in patient A (Fig. 4c). Moreover, the induction of IFN-γ-secreting cells could be detected during Peg-IFN/RBV therapy in patient B (Fig. 4c). The mean numbers of IFN-γ- and IL-10-secreting spots in HBV-dominant dual-infected patients, patients with monoinfection with HBV genotype Bj ($HBeAb^+$), Bj ($HBeAg^+$), C ($HBeAb^+$), C ($HBeAg^+$), or HCV genotype 1b are shown in Fig. 4d. In patient A, HB core antigen (HBcAg)-specific IFN-γ secretion was weaker than that in

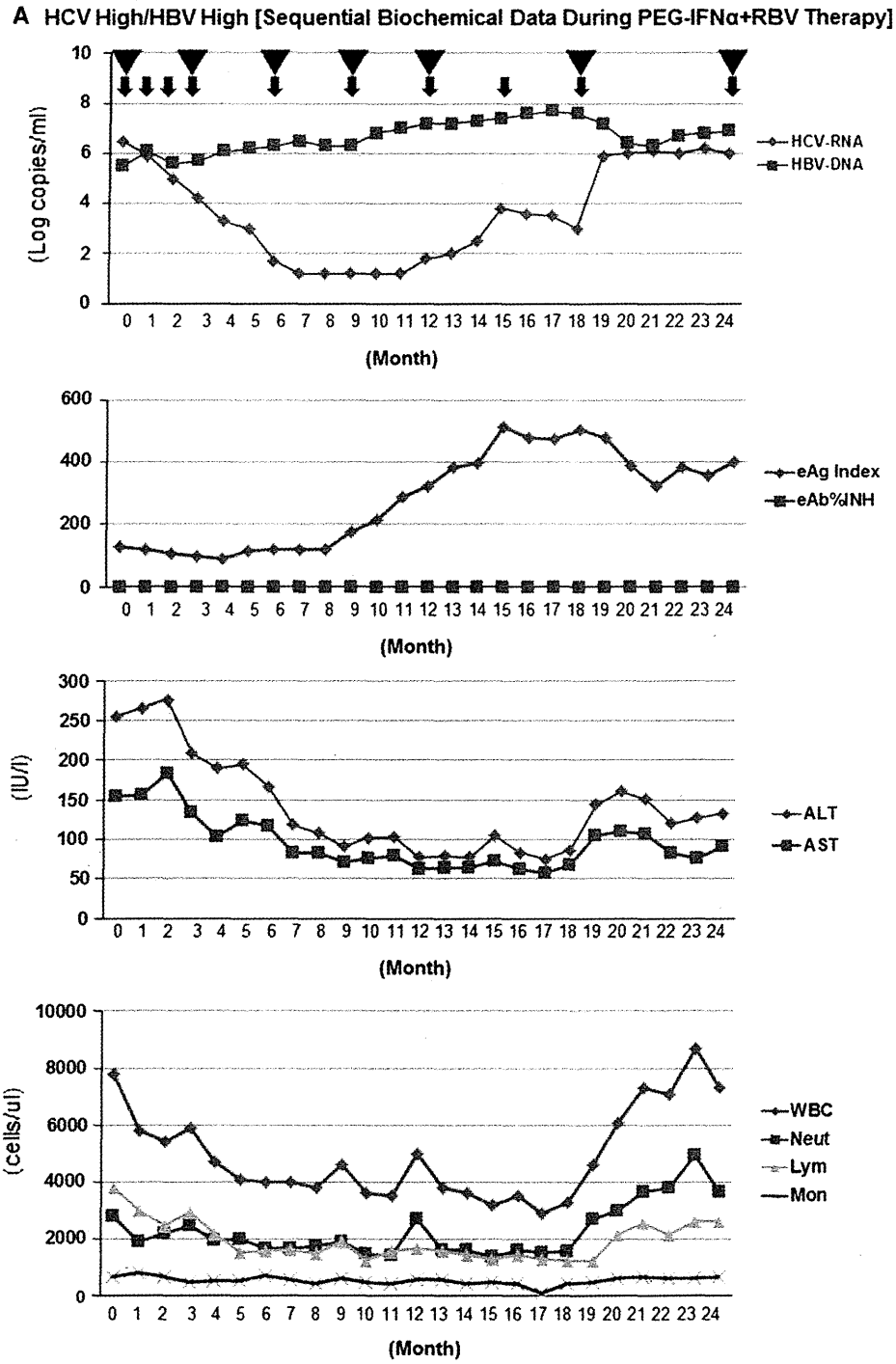

Fig. 3 Sequential biochemical data analysis during Peg-IFN/RBV therapy. The titers of HBV-DNA and HCV-RNA; the amounts of envelope antigen (*eAg*) and envelope antibody (*eAb*), and alanine aminotransferase (*ALT*) and aspartate aminotransferase (*AST*); and the numbers of WBCs, neutrophils (*Neut*), lymphocytes (*Lym*), and monocytes (*Mon*) in patients A (**a**) and B (**b**) are shown in these graphs. *Arrows* indicate the sampling points of FACS analysis. *Triangles* indicate the sampling points of the ELISPOT assay. *INH* inhibition

HBV-genotype C-monoinfected patients who were HBeAg-positive. However, HBcAg-specific IL-10 secretion in patient A was stronger than that in HBV-genotype C monoinfected patients who were HBeAg-positive. These data indicated that the presence of HCV might also suppress the HBV-specific immune response in regard to certain host factors (e.g., in the presence of IL-28B polymorphism, and depending on the body mass index [BMI] and γ-guanosine triphosphate [γ-GTP] level), because the presence of HCV did not suppress the HBV-specific immune response either in patient B or in the patients with dual HCV-dominant infection. Otherwise, we could deny the possibility indicating that

Fig. 3 continued

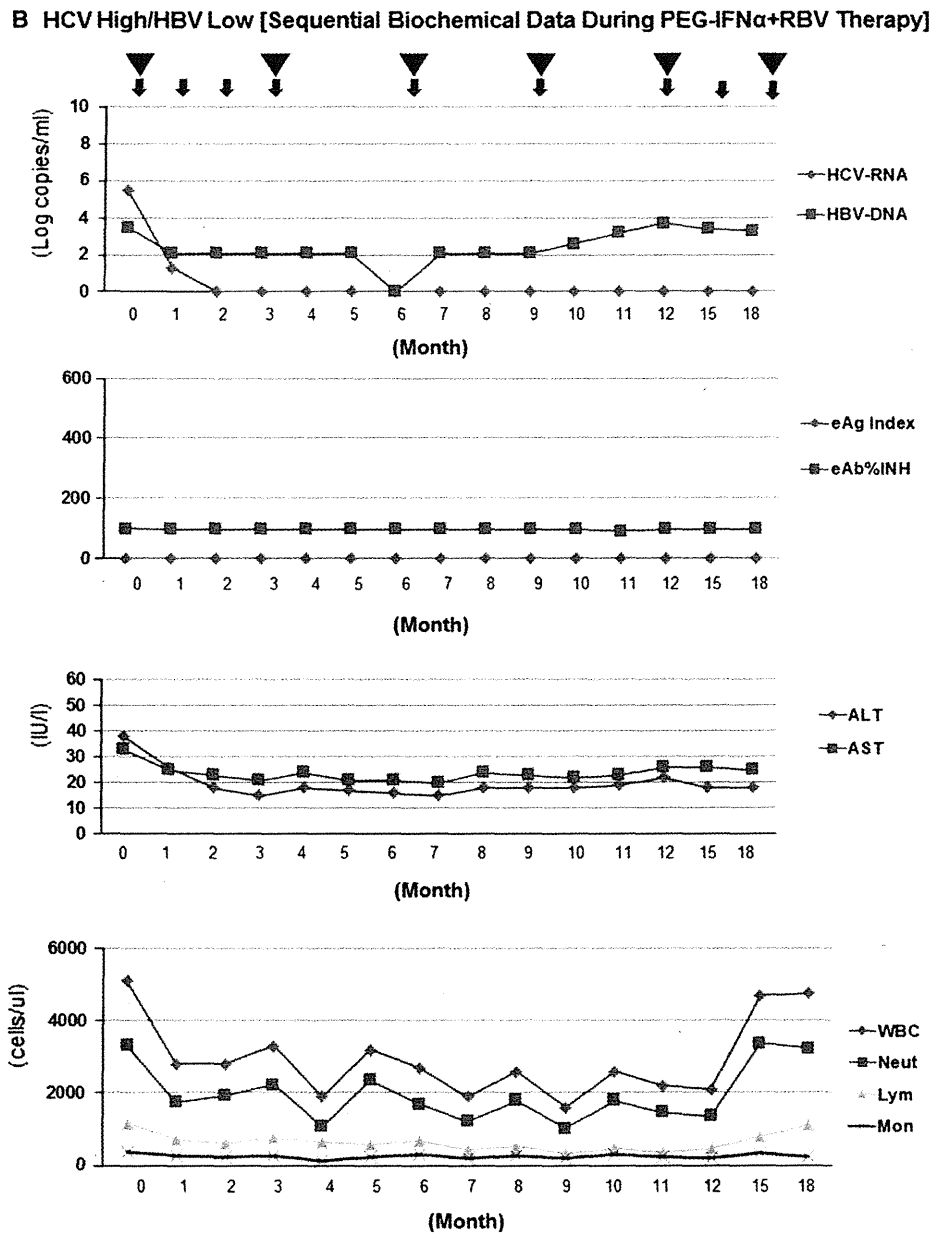

the certain background of host factors could allow the existence of dual virus actively. These data indicated that HBV-specific IL-10-secreting cells and/or certain kinds of host factors had an important role in HBV- and HCV-specific immune suppression in patient A, but not in patient B.

In vitro analysis of HBV/HCV dual infection

We carried out in vitro analysis of HBV/HCV infection using Huh-7 cells that were susceptible to the HCV-JFH-1 strain and HBV expression plasmids. The amount of the JFH-1 strain did not change with the various kinds of HBV expression plasmids (Fig. 5a). Moreover, the amounts of the various HBV strains did not change in the presence of JFH-1 infection. These data indicated that no direct effect of HBV and HCV could be detected in Huh 7 cells. We carried out experiments to analyze the effect of IFN-α treatment on HCV Huh-7 cells with various kinds of HBV expression (Fig. 5b). In our systems, it appeared that HBV expression could not significantly affect the suppressive effect of IFN-α.

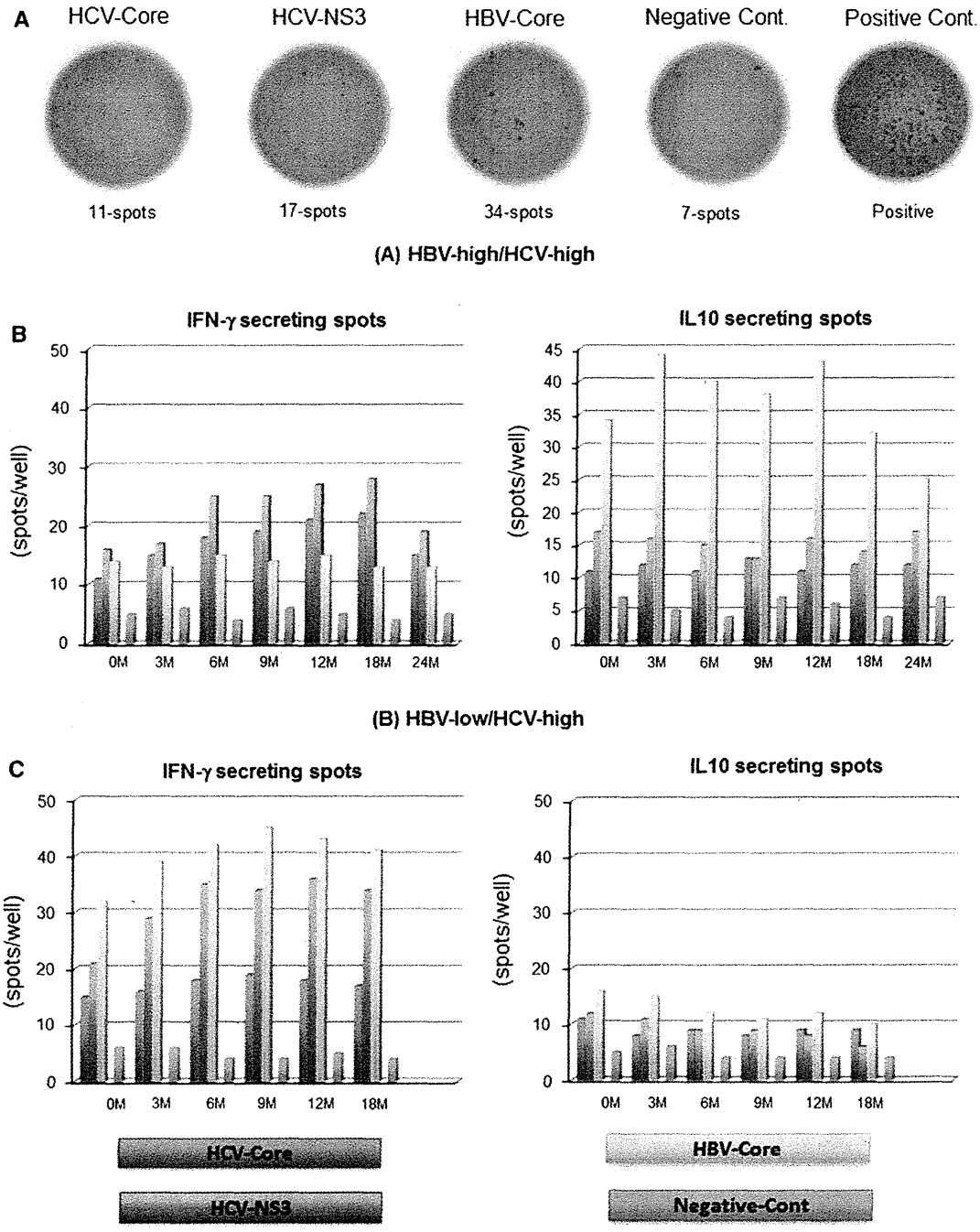

Fig. 4 The sequential analysis of HBV/HCV-specific immune reactions during Peg-IFN/RBV therapy. Representative spots of the ELISPOT assay are shown (**a**). The sequential data of IFN-γ- and interleukin-10 (*IL-10*)- secreting spots in patient A are shown (**b**). The sequential data of IFN-γ- and IL-10-secreting spots in patient B are shown (**c**). Comparison of IFN-γ- and IL-10- secreting spots in patient A before starting therapy, patient B before starting therapy, dual HCV-dominant patients, HCV-monoinfected patients, HBV-Bj ($HBeAb^+$) monoinfected patients, HBV-Bj ($HBeAg^+$) monoinfected patients, HBV-C ($HBeAb^+$) monoinfected patients, and HBV-C ($HBeAg^+$) monoinfected patients (**d**). In these *bar graphs*, the *blue bars* indicate HCV-core specific reaction. The *red bars* indicate HCV-NS3 specific reaction. The *green bars* indicate HBV-core specific reaction. The *aqua blue bars* indicate the negative control (*Cont.*). *Error bars* indicate standard deviations (color figure online)

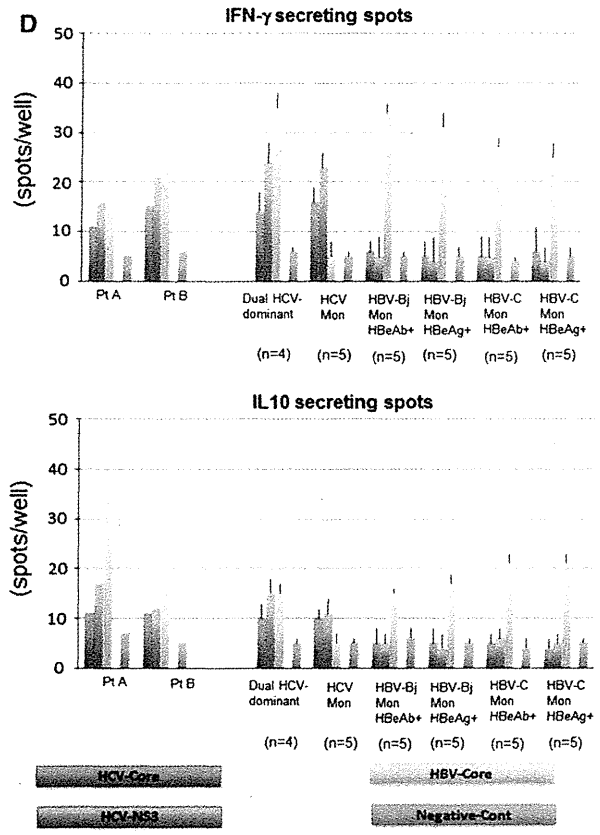

Fig. 4 continued

Discussion

The immunopathogenesis of dual hepatitis B and C infection is not clear, given the complexity of viral and host factors [19, 21, 48–50]. However, detailed understanding of specific patients with dual hepatitis B and C infection could contribute to improving the treatment and follow up of these patients. Therefore, we focused on two representative patients with HBV/HCV dual infection who received Peg-IFN/RBV therapy.

Concerning the virological results, patient A had genotype 1b, HCV-Core 70 wild-type and low mutation of ISDR HCV and genotype C HBV. It has been reported that genotype 1b HCV is common in Japan and is usually difficult to treat in comparison to genotypes 2a and 2b [51]. Among genotype 1b HCV strains, HCV-Core 70 wild-type HCV is easily decreased by Peg-IFN/RBV therapy [51]. On the other hand, it has been reported that in genotype 1b HCV low mutation of ISDR is difficult to treat [52]. Patient B had almost the same background of HCV–genotype 1b, HCV-Core 70 wild-type, and low mutation of ISDR–as patient A. However, the background of host factors that could affect the responsiveness of IFN-based therapy was different between patients A and B. For example, patient A had a hetero allele of the IL-28B polymorphism, advanced fibrosis, and fatty changes of the liver. On the other hand, patient B had the major allele of the IL-28B polymorphism and mild fibrosis. Moreover, the background of HBV in patient B was completely different from that in patient A. It has been reported that HBV genotype Bj is usually more susceptible to IFN-based therapy than genotype C [45, 53]. Therefore, not only the HBV factors but also the combination of host factors and HBV factors might affect the responsiveness to IFN-based therapy. In patient A, the responsiveness of HCV during Peg-IFN/RBV therapy was relatively poor. However, the viral titers of HCV were lower than 1.2 log copies/ml at 7 months after the start of therapy. During the reduction of the HCV viral titers, the titers of HBV and HBc-Ag specific IL-10-secreting cells were gradually increased. Although patient A had received Peg-IFN/RBV therapy for up to 18 months, HCV-RNA increased again 12 months after the start of the therapy. The sustained Th1 immune suppression might have contributed to the relapse of HCV. Not only weak up-regulation of HCV-specific Th1 immune reaction but also strong up-regulation of HBV-specific IL-10-secreting activity was detected during Peg-IFN/RBV therapy in patient A [26, 35]. Moreover, increased HBeAg could be detected 9 months after the start of the therapy. Fluctuations of activated CD4 cells, CD8 cells, NK cells, and NK-T cells could be seen in patient A. On the other hand, in patient B, the responsiveness of HBV and HCV during Peg-IFN/RBV therapy was good. Moreover, the immune response of patient B was almost comparable to the responses in the patients with HCV monoinfection and those with HBV-genotype Bj monoinfection. Previously, it has been reported that Peg-IFN/RBV therapy could achieve almost the same SVR rates in patients with HCV/HBV dual infection and those with HCV monoinfection [54–56]. We assume that the results in these studies were obtained from patients similar to our patient B, because the number of patients with HCV-dominant infection is much higher than the number of those with HBV/HCV dual active infection such as our patient A. Patients with HBV/HCV dual active infection such as patient A are relatively rare in Japan. However, it is necessary to understand the immunopathogenesis of these patients, because Peg-IFN/RBV therapy might not be sufficient to eradicate or control HBV/HCV in these difficult-to-treat patients. One of the candidate therapies for such patients might be Entecavir (ETV)/Peg-IFN/RBV sequential therapy. The effect of HBV specific regulatory T cells might contribute to the immunosuppression of not only HBV but also HCV [35]. In some previous studies, including ours, it has been reported that HBV replication might contribute to immune suppression [19, 29].

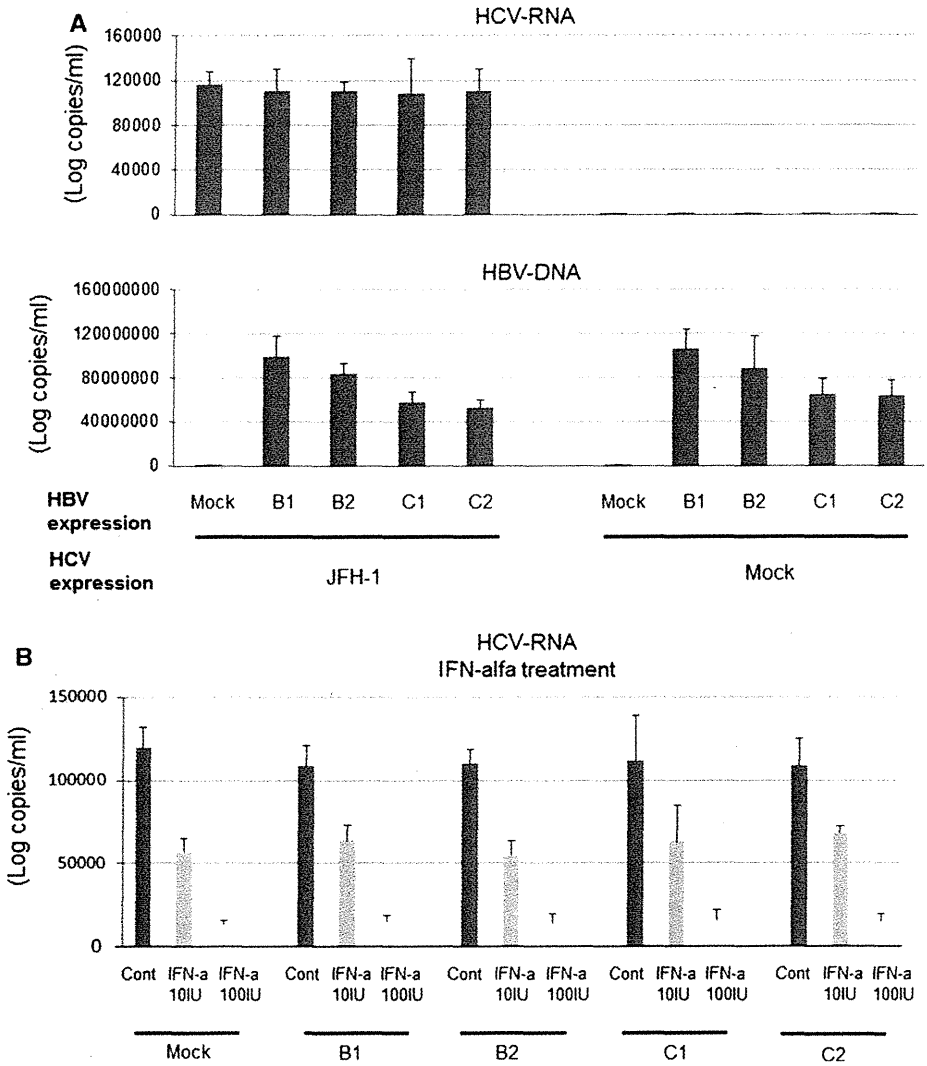

Fig. 5 In vitro analysis of HBV/HCV dual infection. The titers of HCV-RNA and HBV-DNA are shown. *B1* indicates genotype Bj35 clone. *B2* indicates genotype Bj56 clone. *C1* indicates genotype C-AT clone. *C2* indicates genotype C-22 clone (**a**). The titers of HCV-RNA after the IFN-α treatment are shown (**b**)

In the present study, we employed an in vitro coinfection system to analyze the direct interaction between HBV and HCV. In our system, we used several different HBV clones, because it is necessary to consider the effects of different genotypes. Although we could not detect the direct interaction of HBV/HCV in our system, we could not exclude the possibility of indirect interaction between cytokines and chemokines produced from virus-infected hepatocytes. We are now analyzing the chemokines produced from hepatoma cells with different HBV genotype clones (ongoing study).

In conclusion, we analyzed data from representative patients with HBV/HCV dual infection sequentially and precisely. Because many different kinds of backgrounds might affect immunoreactions, we focused on representative patients and analyzed the immunological responses extensively. There might be a group of patients with very difficult-to-treat dual infections. We need to understand the immunopathogenesis of such patients to develop the appropriate therapy.

Acknowledgments This work was supported in part by a Grant-in Aid from the Ministry of Education, Culture, Sport, Science, and Technology of Japan (Y.K. #23790761), and grants from the Ministry of Health, Labor, and Welfare of Japan.

Conflict of interest The authors declare that they have no conflict of interest.

References

1. Alter MJ, Kruszon-Moran D, Nainan OV, et al. The prevalence of hepatitis C virus infection in the United States, 1988 through 1994. N Engl J Med. 1999;341(8):556–62.

2. Tiollais P, Pourcel C, Dejean A. The hepatitis B virus. Nature. 1985;317(6037):489–95.
3. Lai CL, Ratziu V, Yuen MF, Poynard T. Viral hepatitis B. Lancet. 2003;362(9401):2089–94.
4. Poynard T, Yuen MF, Ratziu V, Lai CL. Viral hepatitis C. Lancet. 2003;362(9401):2095–100.
5. Potthoff A, Manns MP, Wedemeyer H. Treatment of HBV/HCV coinfection. Expert Opin Pharmacother. 2010;11(6):919–28.
6. Chu CJ, Lee SD. Hepatitis B virus/hepatitis C virus coinfection: epidemiology, clinical features, viral interactions and treatment. J Gastroenterol Hepatol. 2008;23(4):512–20.
7. Bini EJ, Perumalswami PV. Hepatitis B virus infection among American patients with chronic hepatitis C virus infection: prevalence, racial/ethnic differences, and viral interactions. Hepatology. 2010;51(3):759–66.
8. Halima SB, Bahri O, Maamouri N, et al. Serological and molecular expression of hepatitis B infection in patients with chronic hepatitis C from Tunisia, North Africa. Virol J. 2010;7:229.
9. Saravanan S, Velu V, Nandakumar S, et al. Hepatitis B virus and hepatitis C virus dual infection among patients with chronic liver disease. J Microbiol Immunol Infect. 2009;42(2):122–8.
10. Lee LP, Dai CY, Chuang WL, et al. Comparison of liver histopathology between chronic hepatitis C patients and chronic hepatitis B and C-coinfected patients. J Gastroenterol Hepatol. 2007;22(4):515–7.
11. Liu Z, Hou J. Hepatitis B virus (HBV) and hepatitis C virus (HCV) dual infection. Int J Med Sci. 2006;3(2):57–62.
12. Tsai JF, Jeng JE, Ho MS, et al. Effect of hepatitis C and B virus infection on risk of hepatocellular carcinoma: a prospective study. Br J Cancer. 1997;76(7):968–74.
13. Cho LY, Yang JJ, Ko KP, et al. Coinfection of hepatitis B and C viruses and risk of hepatocellular carcinoma: systematic review and meta-analysis. Int J Cancer. 2011;128(1):176–84.
14. Huo TI, Huang YH, Hsia CY, et al. Characteristics and outcome of patients with dual hepatitis B and C-associated hepatocellular carcinoma: are they different from patients with single virus infection? Liver Int. 2009;29(5):767–73.
15. Kew MC. Interaction between hepatitis B and C viruses in hepatocellular carcinogenesis. J Viral Hepat. 2006;13(3):145–9.
16. Liu CJ, Chen PJ, Chen DS. Dual chronic hepatitis B virus and hepatitis C virus infection. Hepatol Int. 2009;3(4):517–25.
17. Bellecave P, Gouttenoire J, Gajer M, et al. Hepatitis B and C virus coinfection: a novel model system reveals the absence of direct viral interference. Hepatology. 2009;50(1):46–55.
18. Eyre NS, Phillips RJ, Bowden S, et al. Hepatitis B virus and hepatitis C virus interaction in Huh-7 cells. J Hepatol. 2009;51(3):446–57.
19. Chisari FV, Ferrari C. Hepatitis B virus immunopathogenesis. Annu Rev Immunol. 1995;13:29–60.
20. Koziel MJ. The role of immune responses in the pathogenesis of hepatitis C virus infection. J Viral Hepat. 1997;4(Suppl 2):31–41.
21. Rice CM, Walker CM. Hepatitis C virus-specific T lymphocyte responses. Curr Opin Immunol. 1995;7(4):532–8.
22. Nan XP, Zhang Y, Yu HT, et al. Circulating $CD4^{+}CD25^{high}$ regulatory T cells and expression of PD-1 and BTLA on $CD4^{+}$ T cells in patients with chronic hepatitis B virus infection. Viral Immunol. 2010;23(1):63–70.
23. Kondo Y, Ueno Y, Shimosegawa T. Immunopathogenesis of hepatitis B persistent infection: implications for immunotherapeutic strategies. Clin J Gastroenterol. 2009;2(2):71–9.
24. Peng G, Li S, Wu W, Sun Z, Chen Y, Chen Z. Circulating $CD4^{+}$ $CD25^{+}$ regulatory T cells correlate with chronic hepatitis B infection. Immunology. 2008;123(1):57–65.
25. Maier H, Isogawa M, Freeman GJ, Chisari FV. PD-1:PD-L1 interactions contribute to the functional suppression of virus-specific $CD8^{+}$ T lymphocytes in the liver. J Immunol. 2007;178(5):2714–20.
26. Kondo Y, Kobayashi K, Ueno Y, et al. Mechanism of T cell hyporesponsiveness to HBcAg is associated with regulatory T cells in chronic hepatitis B. World J Gastroenterol. 2006;12(27):4310–7.
27. Stoop JN, van der Molen RG, Baan CC, et al. Regulatory T cells contribute to the impaired immune response in patients with chronic hepatitis B virus infection. Hepatology. 2005;41(4):771–8.
28. Kondo Y, Kobayashi K, Asabe S, et al. Vigorous response of cytotoxic T lymphocytes associated with systemic activation of CD8 T lymphocytes in fulminant hepatitis B. Liver Int. 2004;24(6):561–7.
29. Kondo Y, Asabe S, Kobayashi K, et al. Recovery of functional cytotoxic T lymphocytes during lamivudine therapy by acquiring multi-specificity. J Med Virol. 2004;74(3):425–33.
30. Kondo Y, Ueno Y, Kakazu E, et al. Lymphotropic HCV strain can infect human primary naive CD4(+) cells and affect their proliferation and IFN-gamma secretion activity. J Gastroenterol. 2011;46:232–41.
31. Kondo Y, Machida K, Liu HM, et al. Hepatitis C virus infection of T cells inhibits proliferation and enhances fas-mediated apoptosis by down-regulating the expression of CD44 splicing variant 6. J Infect Dis. 2009;199(5):726–36.
32. Kondo Y, Sung VM, Machida K, Liu M, Lai MM. Hepatitis C virus infects T cells and affects interferon-gamma signaling in T cell lines. Virology. 2007;361(1):161–73.
33. Ulsenheimer A, Gerlach JT, Gruener NH, et al. Detection of functionally altered hepatitis C virus-specific CD4 T cells in acute and chronic hepatitis C. Hepatology. 2003;37(5):1189–98.
34. Cramp ME, Rossol S, Chokshi S, Carucci P, Williams R, Naoumov NV. Hepatitis C virus-specific T-cell reactivity during interferon and ribavirin treatment in chronic hepatitis C. Gastroenterology. 2000;118(2):346–55.
35. Kondo Y, Ueno Y, Kobayashi K, et al. Hepatitis B virus replication could enhance regulatory T cell activity by producing soluble heat shock protein 60 from hepatocytes. J Infect Dis. 2010;202(2):202–13.
36. Nguyen LH, Ko S, Wong SS, et al. Ethnic differences in viral dominance patterns in patients with hepatitis B virus and hepatitis C virus dual infection. Hepatology. 2011;53(6):1839–45.
37. Takahashi M, Nishizawa T, Gotanda Y, et al. High prevalence of antibodies to hepatitis A and E viruses and viremia of hepatitis B, C, and D viruses among apparently healthy populations in Mongolia. Clin Diagn Lab Immunol. 2004;11(2):392–8.
38. Ina Y. ODEN: a program package for molecular evolutionary analysis and database search of DNA and amino acid sequences. Comput Appl Biosci. 1994;10(1):11–2.
39. Thompson JD, Higgins DG, Gibson TJ. CLUSTAL W: improving the sensitivity of progressive multiple sequence alignment through sequence weighting, position-specific gap penalties and weight matrix choice. Nucleic Acids Res. 1994;22(22):4673–80.
40. Saitou N, Nei M. The neighbor-joining method: a new method for reconstructing phylogenetic trees. Mol Biol Evol. 1987;4(4):406–25.
41. Felsenstein J. Estimating effective population size from samples of sequences: a bootstrap Monte Carlo integration method. Genet Res. 1992;60(3):209–20.
42. Perriere G, Gouy M. WWW-query: an on-line retrieval system for biological sequence banks. Biochimie. 1996;78(5):364–9.
43. Wakita T, Pietschmann T, Kato T, et al. Production of infectious hepatitis C virus in tissue culture from a cloned viral genome. Nat Med. 2005;11(7):791–6.
44. Takeuchi T, Katsume A, Tanaka T, et al. Real-time detection system for quantification of hepatitis C virus genome. Gastroenterology. 1999;116(3):636–42.

45. Sugauchi F, Kumada H, Sakugawa H, et al. Two subtypes of genotype B (Ba and Bj) of hepatitis B virus in Japan. Clin Infect Dis. 2004;38(9):1222–8.
46. Sugauchi F, Orito E, Ichida T, et al. Epidemiologic and virologic characteristics of hepatitis B virus genotype B having the recombination with genotype C. Gastroenterology. 2003; 124(4):925–32.
47. Orito E, Mizokami M, Sakugawa H, et al. A case–control study for clinical and molecular biological differences between hepatitis B viruses of genotypes B and C. Japan HBV Genotype Research Group. Hepatology. 2001;33(1):218–23.
48. Raimondo G, Brunetto MR, Pontisso P, et al. Longitudinal evaluation reveals a complex spectrum of virological profiles in hepatitis B virus/hepatitis C virus-coinfected patients. Hepatology. 2006;43(1):100–7.
49. Chuang WL, Dai CY, Chang WY, et al. Viral interaction and responses in chronic hepatitis C and B coinfected patients with interferon-alpha plus ribavirin combination therapy. Antivir Ther. 2005;10(1):125–33.
50. Tsai SL, Liaw YF, Yeh CT, Chu CM, Kuo GC. Cellular immune responses in patients with dual infection of hepatitis B and C viruses: dominant role of hepatitis C virus. Hepatology. 1995;21(4):908–12.
51. Akuta N, Suzuki F, Hirakawa M, et al. Amino acid substitution in hepatitis C virus core region and genetic variation near the interleukin 28B gene predict viral response to telaprevir with peginterferon and ribavirin. Hepatology. 2010;52(2):421–9.
52. Fukuma T, Enomoto N, Marumo F, Sato C. Mutations in the interferon-sensitivity determining region of hepatitis C virus and transcriptional activity of the nonstructural region 5A protein. Hepatology. 1998;28(4):1147–53.
53. Akuta N, Kumada H. Influence of hepatitis B virus genotypes on the response to antiviral therapies. J Antimicrob Chemother. 2005;55(2):139–42.
54. Yu ML, Lee CM, Chuang WL, et al. HBsAg profiles in patients receiving peginterferon alfa-2a plus ribavirin for the treatment of dual chronic infection with hepatitis B and C viruses. J Infect Dis. 2010;202(1):86–92.
55. Yu JW, Sun LJ, Zhao YH, Kang P, Gao J, Li SC. Analysis of the efficacy of treatment with peginterferon alpha-2a and ribavirin in patients coinfected with hepatitis B virus and hepatitis C virus. Liver Int. 2009;29(10):1485–93.
56. Liu CJ, Chuang WL, Lee CM, et al. Peginterferon alfa-2a plus ribavirin for the treatment of dual chronic infection with hepatitis B and C viruses. Gastroenterology. 2009;136((2)):496.e3–504.e3.